

# Cancellation of $1/m_Q$ Corrections to the Inclusive Decay Width of a Heavy Quark.

A. Sinkovics, R. Akhoury and V. I. Zakharov

*The Randall Laboratory of Physics  
University of Michigan  
Ann Arbor, MI 48109-1120*

## Abstract

We consider the infrared sensitivity of the inclusive heavy quark decay width in perturbation theory. It is shown by explicit calculations to the second loop order (when the non-abelian nature of the QCD interactions first become apparent) that all infrared sensitive terms to logarithmic and linear accuracy cancel when the decay width is expressed in terms of the short distance mass. This in turn implies the absence of any non perturbative  $1/m_Q$  power corrections to the decay width. The cancellation is shown algebraically at the level of the Feynman integrands without any use of an explicit infrared cutoff. This result is in accord with the implications of the KLN theorem.

## I. INTRODUCTION

The theory of heavy quark decays has attracted much interest lately in connection with the decays of B mesons containing a single b-quark. Of particular phenomenological interest are the inclusive decays which can provide information about the CKM parameters. Inclusive decays of hadrons containing a single heavy quark (mass  $m_b$ ) have been extensively studied [1] within the operator product expansion (OPE) which gives an expansion of the decay width in terms of a small parameter  $\Lambda/m_b$  :

$$\Gamma_{incl} = \Gamma_{incl}^{pert}(1 + a_1\Lambda/m_b + a_2(\Lambda/m_b)^2 + \dots). \quad (1)$$

In the above,  $\Gamma_{incl}^{pert}$  is the decay width of the heavy quark including all perturbative corrections (the parton model result). Since there are no local gauge invariant operators of the appropriate dimension, an important conclusion [1] is that  $a_1 = 0$ , and the higher order power corrections can be classified in terms of the matrix elements of various operators.

A great advantage of the OPE is the generality of its applicability to non-perturbative contributions as well. On the other hand, the conditions for the validity of the OPE itself can be enunciated by explicit perturbative calculations. As far as the power corrections are concerned, the method of renormalons (for a review and further references see [2]) may be used to study these within perturbation theory. The basic idea of the renormalon method is that one may obtain information about power corrections by looking at a class of diagrams which give factorial divergence in large orders of perturbation theory. The power corrections are seen to arise from regions of low momenta and thus we are led to investigate the infrared sensitivity of inclusive decays. To this end  $\Lambda$ , which is a non-perturbative parameter is replaced by an infrared cutoff defined within perturbation theory. We will generically denote this infrared cutoff by  $\lambda$  and in the case of QED, for example, it could be a (fictitious) photon mass. Then the inclusive rate (1) may be represented as :

$$\Gamma_{incl} = \Gamma_{incl}^{pert}(1 + b_1\lambda/m_b + b_2(\lambda/m_b)^2\ln\lambda + \dots). \quad (2)$$

Note that the Landau conditions for the singularities of Feynman diagrams tell us that the infrared sensitive contributions arise only as terms which are non-analytic in  $\lambda^2$ . Explicit calculations [3] to leading order in  $\alpha$  have brought to light a subtlety that the coefficient  $b_1$  is zero in perturbation theory only if the decay rate on the right hand side of Eq. (2) is expressed not in terms of the pole mass  $m_b$  but rather in terms of a short distance or a  $\bar{M}S$  mass. Thus perturbation theory is in full accord with the OPE, only if in (1) the short distance mass is used. In this way one does not have to worry about an otherwise large (possibly non-universal) correction of order  $1/m_b$ , but only at the expense of introducing a renormalization scale ( $\mu$ ) dependence in the total rate through the use of the running mass. We will discuss below that this result arises from the cancellation of the infrared sensitive contributions proportional to  $\lambda/m_b$  (and of course to  $\ln\lambda$ ) arising from the long distance pieces of the mass and wave function renormalizations of the initial heavy quark and from the gluon radiation.

The result mentioned at the end of the previous paragraph has a simple physical interpretation. The decay rate may have two possible sources [4] of infrared sensitivity : (a) the heavy quark mass and (b) the energy radiated during the decay. To expose the infrared

sensitivity of the heavy quark mass say within QED, consider a  $Q\bar{Q}$  pair separated by a distance  $r$  and interacting by the exchange of photons of mass  $\lambda$ . The total energy is

$$E = 2m_b - \frac{\alpha_{el}}{r} \exp(-\lambda r) \sim 2m_b \left(1 + \frac{\alpha_{el}\lambda}{2m_b}\right) - \alpha_{el}/r \quad (3)$$

where we have kept only the term linear in  $\lambda$ . It is clear from this that we may identify

$$m_b^{IR} = \alpha_{el}\lambda/2, \quad (4)$$

with the infrared sensitive piece of the heavy quark mass and for small  $r$  it is appropriate to define the short distance mass  $\bar{m}$  by:

$$\bar{m} = m_b \left(1 + \frac{\alpha_{el}\lambda}{2m_b}\right) \quad (5)$$

The same result was obtained in [3] by the usual renormalon method. Let us next consider the radiated energy. If the decay time is  $\tau$  then classically, a light signal cannot reach a distance beyond

$$R_{causal} = c \cdot \tau \quad (6)$$

As a result, the field energy stored at distances larger than  $R_{causal}$  cannot be transformed into the energy of the decay products and cannot affect the decay rate and hence must be radiated away. Let us denote this long distance piece of the energy radiated during the decay by  $E_{rad}^{IR}$ . That this long distance part of the radiated energy is proportional linearly to the infrared cutoff may be seen from the classical expression for it:

$$E_{rad}^{IR} = \int_{small \ \omega} d\omega I(\omega). \quad (7)$$

$I(\omega)$  is the intensity of radiation which approaches a constant [5] as  $\omega \rightarrow 0$ . The cancellation of the linear term in Eq. (2) is the statement that to this order,

$$m_b^{IR} = E_{rad}^{IR} \quad (8)$$

and the decay rate which is sensitive to the energy release at short distances is not affected.

Certain questions immediately come to mind concerning the generality of these results. Is there a general principle behind this cancellation?, and is it true to all orders in perturbation theory, even for the non-abelian case? In fact there are infrared safe observables in QCD that do receive power corrections that are proportional to  $1/M$  where  $M$  is a large mass scale. Examples are provided by the event shape variables in  $e^+e^-$  annihilation [6] for which there does not exist an operator product expansion. It has been argued in ref. [7] that inclusive enough observables do not receive power corrections of the type  $1/M$  whereas those that assume some precision measurement (and hence are more exclusive) like the event shapes, in fact do. Below we will apply this general principle to the inclusive decay of the heavy quark. We will argue that the KLN [8] theorem is behind the cancellation of the terms proportional to  $1/m_b$ . The purpose of this paper is to show by an explicit calculation in the full QCD theory the cancellation of the infrared sensitive pieces that are linear in the infrared cutoff to order  $\alpha_s^2$  in the decay rate.

In a recent publication [9] it was argued that when the transition probability is summed over both initial and final degenerate states as is envisaged in the KLN theorem, not only the leading infrared sensitive piece proportional to  $\ln\lambda$  but the one proportional to  $\lambda$  is cancelled as well, i.e.,

$$\sum_{i,f} |S_{i \rightarrow f}|^2 \sim 0 \cdot \ln\lambda + 0 \cdot \lambda + \text{terms independent of } \lambda + O(\lambda^2 \ln\lambda). \quad (9)$$

The transition probability summed over both initial and final states cannot be related to a physical inclusive cross section. However we will now argue that for heavy quark decay, the initial state is trivial and hence, the above mentioned property of the KLN theorem guarantees the cancellation not only of the  $\ln\lambda$  terms but also those proportional to  $\lambda$  itself. To substantiate this we note that the KLN theorem presumes that the total energy can be fixed to any accuracy. This is in the spirit of the uncertainty principle, which allows us to measure the total energy to any accuracy provided the measurement time is long enough. In particular, the uncertainty  $\Delta E$  in the total energy can be made smaller than an infrared cutoff:

$$\Delta E \ll \lambda \quad (10)$$

Now consider a decaying charged (or colored) particle in its rest frame. It is obvious that this state is not degenerate with any other since there is a gap between the mass of the charged particle and the energies in the continuum for any  $\lambda \neq 0$ . This is most clearly seen for QED with a non-zero photon mass, but is true for any infrared cutoff on the energy,  $\lambda$ . Thus the summation over the initial states in the KLN theorem is redundant for this case. The final states however include the full degeneracy but the summation over the final states is equivalent to calculating the decay width, and hence we conclude that,

$$\Gamma_{incl} = \Gamma_{incl}^{pert} (1 + O(\lambda^2 \ln\lambda)). \quad (11)$$

It should be emphasized that this argument guarantees the above equality to all orders in perturbation theory. However we should note that it is very important for the KLN theorem to be valid that the renormalization procedure does not introduce any infrared sensitivity. Thus since the pole mass is infrared sensitive, on shell mass renormalization must be avoided in favour of the  $\bar{M}\bar{S}$  scheme. In concluding this we would like to point out that the same argument can be applied not just to the semileptonic decay but to other inclusive decays like for example the radiative one,  $B \rightarrow X_s \gamma$ . In fact, the explicit perturbative calculation though performed for the semileptonic decay, can equally well be applicable for the radiative decay  $b \rightarrow s \gamma$  with minor changes for the electroweak vertices and phase space factors.

As mentioned previously, we will explicitly verify the above argument in this paper for the inclusive semileptonic decay of a heavy quark in QCD to the second loop order when the non-abelian nature of the interactions are first apparent. That is we show the cancellations of all terms linear in the infrared cutoff in the decay width when the latter is expressed in terms of the short distance mass. The possible sources of infrared sensitive terms are the mass and wave function renormalization diagrams of the initial heavy quark and the bremsstrahlung diagrams. We will discuss the cancellation of the logarithmic and the linearly infrared sensitive terms in the diagrams for the wave function renormalization and of the linearly

IR sensitive terms in those for the mass renormalization. These cancellations proceed in a different manner for the two cases because whereas the wave function renormalization is multiplicative, the on-mass shell renormalization is additive. In section II we introduce our notations and conventions and discuss our strategy. In particular we show how to the linear accuracy desired, we may replace the diagrams for the radiation from the final state massless quark by effective local vertices. Next we discuss the wave function renormalization in section III and the mass renormalization in section IV. Certain additional technical details are relegated to the appendix. In section V we summarize our results and discuss future prospects.

## II. PRELIMINARIES

We consider the totally inclusive semileptonic decay of a heavy quark and examine the possible term linearly proportional to an infrared cutoff. Such a term can arise from the soft gluon contributions to the diagrams for the mass and wave function renormalizations of the heavy quark and from the bremsstrahlung diagrams.

The decay rate is proportional to the imaginary part of the forward amplitude shown in Fig. 1. The hard amplitude involving the final state quark is denoted by the shaded blob which also includes the lepton loop. The soft gluon interactions responsible for the infrared sensitivity dress the hard amplitude, connecting to it and to the heavy quark. We will use the fact that for the soft gluon of momenta  $k \ll m_b$ , we may perform the sum over cuts implicit in taking the imaginary part, for just the hard part of the amplitude leaving the soft gluon lines uncut. This simplification arises due to the fact that for the process of a heavy quark decay, we may assign a positive energy flow direction to each soft gluon consistently. Then we may write for the corresponding gluon propagator:

$$\frac{i}{k^2 + i\epsilon} = 2\pi\theta(k_0)\delta(k^2) + \frac{i}{k^2 + ik_0\epsilon} \quad (12)$$

The second term can never cause a pinch singular point since the contour can be deformed into the lower half  $k_0$  plane. This piece therefore (from the Landau equations) does not give any contributions that are non-analytic in the infrared cutoff. Thus as far as the infrared sensitive terms are concerned, even upto linear accuracy it does not matter if we cut the gluon propagator or not, both possibilities giving the same contribution. Keeping this in mind, we will sum over the cuts of the hard amplitude only and leave the soft gluon propagators uncut in the diagrams for the forward scattering amplitude. The next simplification of the forward scattering amplitude we will use for our infrared analysis is that the (heavy quark) propagators on the right hand side of the cut can also be taken to have the  $+i\epsilon$  prescription, the same as those on the left hand side of the cut. The difference between the two choices is readily seen to be pure imaginary and since the cut hard amplitude is already imaginary, we may ignore this difference for our purposes.

Let us consider the diagrams with the soft gluon radiation interacting with the hard part. In the next subsection we will show that to the accuracy we want, after summing over the cuts of the hard part, and integrating over its phase space and that of the leptons, this interaction may be replaced by effective local vertices for the interaction of one and two gluons. These effective vertices may be obtained from the corresponding one without

gluon radiation by gauge invariance. Thus we can forget about the details of the hard part and use the effective vertices to discuss the infrared sensitive contributions for such diagrams. Diagrams in which all the gluon interactions are contained in the hard part are irrelevant to our analysis as far as the infrared sensitive terms are concerned which are linearly proportional to the infrared cutoff. Since the wave function renormalization is multiplicative, all its contributions factorize from the hard amplitude. In addition, as we discuss below the corresponding bremsstrahlung diagrams that cancel the logarithmic and linear dependence on the IR cutoff of the wave function renormalization diagrams may be obtained by certain Ward-like identities. These cancellations can be shown independent of the hard amplitude whose precise structure is not needed here, but the latter is essential for showing the cancellations among the mass renormalization and the corresponding radiation type diagrams. The use of the heavy quark rest frame provides very important simplifications of this analysis.

In this paper all the infrared cancellations are shown strictly algebraically at the level of the corresponding Feynman integrands. Power counting is used to isolate and to show the cancellations of the possibly infrared sensitive contributions upto linear accuracy. After the cancellations, from power counting, the integrand is seen to contribute something which would at least be proportional quadratically to the infrared cutoff. In this way we avoid using any particular IR cutoff. This is crucial since for the non-abelian theory we do not know of any gauge invariant infrared cutoff for explicit calculations at the two loop level.

Finally we note that throughout this paper we work in the Feynman gauge. The cancellation of the infrared sensitive terms is a gauge invariant statement, however, the type of diagrams contributing to this cancellation depends on the choice of gauge.

### A. Effective vertices for the Interaction of radiation with the Hard Amplitude

In this section we will derive the effective vertices for the interaction of the gluon radiation with the final state massless quark in the hard amplitude.. These effective local vertices are constructed to reproduce the soft momentum ( $k \ll m_b$ ) contributions upto linear in  $1/m_b$  accuracy. Consider the absorbtion of a single gluon of momentum  $k$  from the final state quark. We will show below that summing over the cuts for the final state fermion line cancels the term proportional to  $1/k$  (i.e., the would be infrared divergent term proportional to  $\ln\lambda$ ) so that the leading left over piece is of order  $k^0$ . When the other end of the gluon line is attached to the heavy quark line then we would be interested in the term proportional to  $\lambda$  and from simple power counting of the corresponding diagram we see that we need only keep this leading term proportional to  $k^0$  from the sum over cuts of the final state quark. In this way we will conclude that after the phase space integration over the leptons and the final state quark at fixed  $k$  this effective interaction may be represented by a local vertex of the form shown in Fig. 3b). We show below that this effective local vertex is what we would obtain by the substitution  $p \rightarrow (p - gA)$  in the leading effective vertex of Fig. 3a). A similar effective vertex is derived for the absorbtion of two gluons from the final state quark. Since as mentioned earlier, the heavy quark wave function renormalization contribution to the infrared sensitivity is multiplicative in nature, these contributions are not sensitive to the details of the interaction of the final state quark and the effective vertices derived in this section are not needed there.

In the parton model, the total width for the semileptonic decay is to lowest order:

$$\Gamma_0 = \frac{G_F^2 |V_{ub}|^2}{192\pi^3} m_b^5 \quad (13)$$

We may represent this by an effective local vertex, obtained by performing the phase space integration over the leptons and the massless quark by the heavy dot in Fig. 3a). Such an effective vertex may be written as:

$$C \bar{u} \not{p}^5 u \quad (14)$$

where,  $u$  is the heavy quark spinor. In the above,

$$C = \frac{G_F^2 |V_{ub}|^2}{192\pi^3}. \quad (15)$$

The vertex of Fig. 3a) will be referred to as the leading effective vertex. Next consider the class of diagrams of Fig. 2a). The gluon may undergo self interactions before connecting to the heavy quark line. Thus, for example, the diagrams of Fig. 2b) are included in the set. Next we sum over the two cuts on the massless quark line. In one just the quark line is cut and in the other, both the quark and gluon lines are cut. However, as discussed above and as it was shown in explicit examples in ref. [9], as far as the infrared sensitive terms (those that are non-analytic in the infrared cutoff) are concerned, both real and virtual soft quanta may be regarded the same i.e, we may write for the gluon line contribution either as  $2\pi\theta(k_0)\delta(k^2)$  or  $i/(k^2+i\epsilon)$ . This is really a consequence of the Landau equations as discussed earlier. Keeping this in mind we can write for the sum over cuts in Fig. 2a) as:

$$- \Gamma^* \not{p}_1 \gamma^\alpha g T^a (\not{p}_1 - \not{k}) \Gamma 2\pi \left[ \frac{\delta(p_1^2)}{(p_1 - k)^2 + i\epsilon} + \frac{\delta((p_1 - k)^2)}{p_1^2 - i\epsilon} \right], \quad (16)$$

where  $\Gamma$  generically denote the weak interaction vertices, and  $p_1 = (p - q)$  with  $q$  the momentum transfer to the leptons. Note that the lepton loop is always cut and we do not explicitly write down the corresponding expression. We also have not explicitly written down the contributions from the blob in Fig. 2a) and those from the external quark lines since their exact form is inessential to the argument. Now we can use the following identity to simplify the term in squared brackets above:

$$\begin{aligned} & \frac{\delta(p_1^2)}{(p_1 - k)^2 + i\epsilon} + \frac{\delta((p_1 - k)^2)}{p_1^2 - i\epsilon} = \\ & (-1) \int_0^1 dx_1 \int_0^1 dx_2 \delta(1 - x_1 - x_2) \delta^{(1)} \left( x_1 p_1^2 + x_2 (p_1 - k)^2 \right). \end{aligned} \quad (17)$$

In the limit  $k \rightarrow 0$  the right hand side of Eq. (17) becomes:

$$(-1) \delta^{(1)}(p_1^2), \quad (18)$$

which is a well defined quantity. This shows the cancellation of the leading infrared divergent term, and the next term in the sum over cuts, which is  $O(k^0)$  may be written as:

$$- \Gamma^* \not{p}_1 \gamma^\alpha g T^a \not{p}_1 \Gamma 2\pi (-1) \delta^{(1)}(p_1^2) \quad (19)$$

We wish to compare this with the corresponding expression for the absorbtion of a zero momentum gluon from the uncut final state massless quark of momentum  $p_1$  which is:

$$i \Gamma^* \not{p}_1 \gamma^\alpha g T^a \not{p}_1 \Gamma \frac{1}{(p_1^2 + i\epsilon)^2}. \quad (20)$$

Using the fact that:

$$2i \text{Im} \frac{1}{(p_1^2 + i\epsilon)^2} = 2\pi \delta^{(1)}(p_1^2), \quad (21)$$

and comparing with Eq. (19) we see that as far as the terms of order  $k^0$  are concerned we may represent the diagram of Fig. 2a) for fixed  $k$  as an effective local interaction which after the appropriate phase space integrations over the leptons and the massless quark for a fixed  $k$  may be obtained from the effective vertex Eq. (14) by means of the replacement  $p_\mu \rightarrow (p_\mu - g T^a A_\mu^a)$ . We have of course shown this only for the one gluon effective vertex shown in Fig. 3b). Next we will show that the same substitution also reproduces the two gluon emission or absorbtion process.

Consider next the absorbtion of two gluons by the final state quark as shown in Fig. 2c) and once again the blob represents all possible interactions and connections of these gluons with each other and with the heavy quark. The sum over cuts of the massless quark line for this configuration for fixed  $k_1, k_2$  is:

$$\begin{aligned} & \Gamma^* \not{p}_1 g T^a \gamma^\alpha (\not{p}_1 - \not{k}_2) g T^b \gamma^\beta (\not{p}_1 - \not{k}_1 - \not{k}_2) \Gamma 2\pi \left[ \delta(p_1^2) \frac{1}{(p_1 - k_2)^2 + i\epsilon} \frac{1}{(p_1 - k_1 - k_2)^2 + i\epsilon} + \right. \\ & \left. \delta((p_1 - k_2)^2) \frac{1}{p_1^2 - i\epsilon} \frac{1}{(p_1 - k_1 - k_2)^2 + i\epsilon} + \delta((p_1 - k_1 - k_2)^2) \frac{1}{p_1^2 - i\epsilon} \frac{1}{(p_1 - k_2)^2 - i\epsilon} \right] \quad (22) \end{aligned}$$

Next we use a generalization of the identity Eq. (17),

$$\begin{aligned} & \delta(p_1^2) \frac{1}{(p_1 - k_2)^2 + i\epsilon} \frac{1}{(p_1 - k_1 - k_2)^2 + i\epsilon} + \delta((p_1 - k_2)^2) \frac{1}{p_1^2 - i\epsilon} \frac{1}{(p_1 - k_1 - k_2)^2 + i\epsilon} + \\ & \delta((p_1 - k_1 - k_2)^2) \frac{1}{p_1^2 - i\epsilon} \frac{1}{(p_1 - k_2)^2 - i\epsilon} = (-1)^2 \int_0^1 \dots \int_0^1 dx_1 dx_2 dx_3 \delta(1 - x_1 - x_2 - x_3) \times \\ & \delta^{(2)}(x_1 p_1^2 + x_2 (p_1 - k_2)^2 + x_3 (p_1 - k_1 - k_2)^2) \quad (23) \end{aligned}$$

The right hand side of (23) tends to a well defined limit as  $k_i \rightarrow 0$ ,

$$(-1)^2 \frac{1}{2} \delta^{(2)}(p_1^2) \quad (24)$$

which again represents the cancellation of the leading logarithmically divergent contribution. The term proportional to  $k^0$  in the sum over cuts is then given by:

$$\Gamma^* \not{p}_1 g T^a \gamma^\alpha \not{p}_1 g T^b \gamma^\beta \not{p}_1 \Gamma (-1)^2 \frac{1}{2} \delta^{(2)}(p_1^2). \quad (25)$$



Again consider the corresponding term for the absorbtion of two zero momentum gluons from the massless quark line:

$$-i\Gamma^*\not{p}_1 g T^a \gamma^\alpha \not{p}_1 g T^b \gamma^\beta \not{p}_1 \Gamma \frac{1}{(p_1^2 + i\epsilon)^3} \quad (26)$$

Since

$$2iIm \frac{1}{(p_1^2 + i\epsilon)^3} = -\pi \delta^{(2)}(p_1^2), \quad (27)$$

comparing with (25) we see that the  $O(k^0)$  contribution from the sum over cuts may again be written as an effective local vertex after the relevant phase space integrations. This local vertex can be obtained from Eq. (14) by means of the replacement  $p_\mu \rightarrow (p_\mu - gT^a A_\mu^a)$  and expanding to  $O(g^2)$ . Note that there is a similar contribution as in Eq.(25) but with the interchange  $(\alpha, a) \leftrightarrow (\beta, b)$ , and this too is reproduced by the above mentioned replacement. The two gluon effective vertex is shown in Fig. 3c).

We should remark here that when we go beyond the two gluon emission case, in general multi-gluon emission or absorbtion from the final state line cannot be written as an effective local vertex. Fortunately this is not a problem for us.

### III. CANCELLATION OF INFRARED SENSITIVE TERMS UPTO LINEAR ACCURACY FROM THE WAVE FUNCTION RENORMALIZATION DIAGRAMS

In this section we will show that the infrared sensitive terms upto linear accuracy are cancelled between the wave function renormalization contributions from diagrams with self energy insertions and parts of other diagrams related to the bremsstrahlung. The cancelling sets can be arranged into groups which as we will see below upto linear accuracy are obtained through certain Ward-like identities. For the cancellations considered in this section which are related to the wave function renormalization, the corresponding contributions are such that the hard part of the diagrams factorize. The hard part thus is not consequential to the argument and just comes along for the ride.

Throughout the paper, we will denote by  $-i\Sigma(p)$  the sum of all 2 point one particle irreducible graphs. Then the full fermion propagator is:

$$S'_F(p) = \frac{i}{\not{p} - m_b - \Sigma(p)} \quad (28)$$

Near the mass shell we have

$$\Sigma(p) = \delta m(m_b, \Delta m) - (Z^{-1} - 1)(\not{p} - m_b) + O((\not{p} - m_b)^2) \quad (29)$$

where  $\Delta m$  denotes the mass counterterm:

$$\delta m(m_b, \Delta m) |_{\not{p}=m_b} = 0. \quad (30)$$

Thus  $m_b$  denotes the pole or the physical mass:

$$\lim_{\not{p} \rightarrow m_b} S'_F(p) = \frac{i}{\not{p} - m_b} Z \quad (31)$$

From the LSZ reduction formula, each external line in the S-matrix element gets a factor  $Z^{1/2}$  and we are interested in its perturbative expansion. Thus we expand,

$$Z^{1/2} = 1 - \frac{1}{2} (Z^{-1} - 1) + \frac{3}{8} (Z^{-1} - 1)^2 + \dots \quad (32)$$

and  $Z^{-1} - 1$  may be computed using:

$$Z^{-1} - 1 = - \frac{\bar{u} \frac{\partial}{\partial p_\nu} \Sigma|_{\not{p}=m_b} u}{\bar{u} \gamma^\nu u} \quad (33)$$

In the rest frame of the heavy quark, only  $\nu = 0$  contributes.

We will now clarify our procedure first with the  $O(\alpha)$  case and next the two loop example will be discussed.

### A. Cancellation to One-Loop Order

Consider the graphs of Fig. 4. The wave function renormalization parts of both graph(a) and graph(b) are the hard part times a factor of  $Z^{1/2}$ . Thus we expand it using (32) keeping only the first two terms and computing the perturbative contribution to order  $\alpha$  of  $Z^{-1} - 1$  from (33). Next using the identity

$$\frac{\partial}{\partial p^\nu} \frac{i}{\not{p} - \not{k} - m_b} = \frac{i}{\not{p} - \not{k} - m_b} i\gamma_\nu \frac{i}{\not{p} - \not{k} - m_b} \quad (34)$$

we obtain the Ward-like identity shown in Fig. 5, where the dotted line just denotes the insertion of a zero momentum vertex  $\gamma_\nu$ . We would now like to show that upto logarithmic and linear accuracy in the infrared, the right hand side of Fig. 5 may be identified with the wave function renormalization part of Fig. 4c) times  $\bar{u}\gamma_\nu u$ , modulo the hard part, which after the relevant phase space integrations just gives a factor of  $Cm_b^5$ . It is easiest to go now to the rest frame of the heavy quark, where

$$\gamma^0 u = u. \quad (35)$$

From this and Eqns. (32), (33) we immediately see

$$4c)|_{\text{wavefunction}} = (Z^{-1} - 1)_{g^2} Cm_b^5 \bar{u}u = -[4a) + 4b)]. \quad (36)$$

Here, and henceforth, unless otherwise specified, the equality sign is for terms that are logarithmically and linearly infrared sensitive. This is the desired result, which does not involve using an explicit infrared cutoff. Let us now see how the wave function renormalization part of Fig. 4c) can be identified with  $(Z^{-1} - 1)_{g^2} Cm_b^5$ , which is effectively the right hand side of Fig. 5 multiplied by the hard part  $Cm_b^5$ . Consider the expressions for these diagrams in the rest frame of the heavy quark. Both are of the form:

$$(ig)^2 C_F C m_b^5 \int \frac{d^4 k}{(2\pi)^4} N \frac{i}{-2pk + k^2} \frac{i}{-2pk + k^2} \frac{-i}{k^2} \quad (37)$$

where  $N$  denotes the numerators  $N_5$  or  $N_{4c}$  for the two diagrams respectively. Thus we only have to compare the numerators to linear accuracy. Upto linear terms in the infrared power counting

$$N_5 = \bar{u} \gamma^\alpha (\not{p} + m) \gamma^0 (\not{p} + m) \gamma_\alpha u - \bar{u} \gamma^\alpha \not{k} \gamma^0 (\not{p} + m) \gamma_\alpha u - \bar{u} \gamma^\alpha (\not{p} + m) \gamma^0 \not{k} \gamma_\alpha u \quad (38)$$

There is a similar expression for the numerator  $N_{4c}$  except for the factor of  $\gamma_0$ . However, using Eq. (35) it is easy to see that to this accuracy the two numerators are equal

$$N_5 = N_{4c} \quad (39)$$

This demonstrates the cancellation of not only the infrared divergent part but also the next linearly infrared sensitive piece in the wave function renormalization. After the cancellation, the integral will be at most quadratically divergent by IR power counting. The cancellation of the wave function parts at two loops follows the same general method except that now we have more diagrams.

## B. Cancellation to Two Loop Order

The 2-loop one particle irreducible diagrams can be divided into 5 groups according to the 5 pieces of the order  $g^4$  self-energy corrections (Fig. 7). These groups are essentially the different color groups, with the exception that the first and third group have the same color structure. In this section we show the cancellation of infrared sensitive terms to linear accuracy in the second loop order for the wave function renormalization diagrams and their radiation counterparts. Power counting in the IR region is used to isolate logarithmically and linearly infrared sensitive pieces of the integrals. In the following, these infrared sensitive terms identified by power counting will be simply referred as “logarithmic and linear pieces” of the corresponding diagrams. As it is discussed below, the cancellation of logarithmic and linear terms takes place within each color group separately. The cancellation is algebraic at the level of integrands and no explicit infrared cutoff is used.

Let us take the second group (Fig. 9) as an example to work with. We would like to show that both the logarithmic and the linear pieces in the wave function renormalization of diagrams 9a) and 9b) cancel the corresponding logarithmic and linear wave function renormalization pieces of diagrams 9c), 9d) and 9e), i.e.

$$\begin{aligned} [9a) + 9b)]_{wavefunction} &= -C m_b^5 (Z^{-1} - 1)_{g^4, \Sigma_{22}} \bar{u} u \\ &= -[9c) + 9d) + 9e)]_{wavefunction} \end{aligned} \quad (40)$$

As before, we may write

$$(Z^{-1} - 1)_{g^4, \Sigma_{22}} = -\frac{\bar{u} \frac{\partial \Sigma_{22}}{\partial p_\nu} \Big|_{\not{p}=m_b} u}{\bar{u} \gamma^\nu u} = -\frac{\bar{u} \frac{\partial \Sigma_{22}}{\partial p_0} \Big|_{\not{p}=m_b} u}{\bar{u} u} \quad (41)$$

where the last equality holds in the rest frame of the heavy quark  $p = (m_b, 0, 0, 0)$ .

We would like to show that to linear accuracy

$$Cm_b^5 \bar{u} \left. \frac{\partial \Sigma_{22}}{\partial p^0} \right|_{\not{p}=m_b} u = iCm_b^5 \bar{u} \left. \frac{\partial(-i\Sigma_{22})}{\partial p^0} \right|_{\not{p}=m_b} u = -[9c) + 9d) + 9e)]_{wavefunction} \quad (42)$$

Since

$$\frac{\partial}{\partial p_0} \frac{i}{\not{p} - \not{k} - m} = \frac{i}{\not{p} - \not{k} - m} i\gamma^0 \frac{i}{\not{p} - \not{k} - m} \quad (43)$$

the derivation of  $\Sigma_{22}$  with respect to  $p_0$  results in the insertion of an extra vertex  $i\gamma^0$  and an extra propagator in every possible way. The resulting diagrams are similar to the wave function renormalization parts of 9c), 9d) and 9e) with the  $Cm_b^5$  vertex replaced by  $-Cm_b^5\gamma^0$  (see Fig. 13b). Writing out explicitly

$$\begin{aligned} Cm_b^5 \bar{u} \left. \frac{\partial \Sigma_{22}}{\partial p_0} \right|_{\not{p}=m_b} u = & -Cm_b^5 \left( C_F^2 - \frac{C_F C_A}{2} \right) (ig)^4 \times \left\{ \int d^4k d^4k_1 N_1 \frac{i}{-2pk + k^2} \times \right. \\ & \frac{i}{-2pk + k^2} \frac{i}{-2p(k + k_1) + (k + k_1)^2} \frac{i}{-2pk_1 + k_1^2} \frac{-i - i}{k^2 k_1^2} + \int d^4k d^4k_1 N_2 \times \\ & \frac{i}{-2pk + k^2} \frac{i}{-2p(k + k_1) + (k + k_1)^2} \frac{i}{-2p(k + k_1) + (k + k_1)^2} \frac{i}{-2pk_1 + k_1^2} \frac{-i - i}{k^2 k_1^2} \\ & + \int d^4k d^4k_1 N_3 \frac{i}{-2pk + k^2} \frac{i}{-2p(k + k_1) + (k + k_1)^2} \frac{i}{-2pk_1 + k_1^2} \frac{i}{-2pk_1 + k_1^2} \\ & \left. \frac{-i - i}{k^2 k_1^2} \right\} \end{aligned} \quad (44)$$

where  $N_1, N_2, N_3$  are the numerator factors

$$\begin{aligned} N_1 &= \bar{u} \gamma^\alpha (\not{p} - \not{k} + m) \gamma^0 (\not{p} - \not{k} + m) \gamma^\beta (\not{p} - \not{k} - \not{k}_1 + m) \gamma_\alpha (\not{p} - \not{k}_1 + m) \gamma_\beta u \\ N_2 &= \bar{u} \gamma^\alpha (\not{p} - \not{k} + m) \gamma^\beta (\not{p} - \not{k} - \not{k}_1 + m) \gamma^0 (\not{p} - \not{k} - \not{k}_1 + m) \gamma_\alpha (\not{p} - \not{k}_1 + m) \gamma_\beta u \\ N_3 &= \bar{u} \gamma^\alpha (\not{p} - \not{k} + m) \gamma^\beta (\not{p} - \not{k} - \not{k}_1 + m) \gamma_\alpha (\not{p} - \not{k}_1 + m) \gamma^0 (\not{p} - \not{k}_1 + m) \gamma_\beta u \end{aligned} \quad (45)$$

Comparing this with diagrams 9c), 9d) and 9e)

$$\begin{aligned} -9c) &= -Cm_b^5 \left( C_F^2 - \frac{C_F C_A}{2} \right) (ig)^4 \int d^4k d^4k_1 N_{1c} \frac{i}{-2pk + k^2} \times \\ & \frac{i}{-2pk + k^2} \frac{i}{-2p(k + k_1) + (k + k_1)^2} \frac{i}{-2pk_1 + k_1^2} \frac{-i - i}{k^2 k_1^2} \\ -9d) &= -Cm_b^5 \left( C_F^2 - \frac{C_F C_A}{2} \right) (ig)^4 \int d^4k d^4k_1 N_{2d} \frac{i}{-2pk + k^2} \times \\ & \frac{i}{-2p(k + k_1) + (k + k_1)^2} \frac{i}{-2p(k + k_1) + (k + k_1)^2} \frac{i}{-2pk_1 + k_1^2} \frac{-i - i}{k^2 k_1^2} \\ -9e) &= -Cm_b^5 \left( C_F^2 - \frac{C_F C_A}{2} \right) (ig)^4 \int d^4k d^4k_1 N_{3e} \frac{i}{-2pk + k^2} \times \\ & \frac{i}{-2p(k + k_1) + (k + k_1)^2} \frac{i}{-2pk_1 + k_1^2} \frac{i}{-2pk_1 + k_1^2} \frac{-i - i}{k^2 k_1^2} \end{aligned} \quad (46)$$

with the numerator factors

$$\begin{aligned}
N_{1c} &= \bar{u} \gamma^\alpha (\not{p} - \not{k} + m) (\not{p} - \not{k} + m) \gamma^\beta (\not{p} - \not{k} - \not{k}_1 + m) \gamma_\alpha (\not{p} - \not{k}_1 + m) \gamma_\beta u \\
N_{2d} &= \bar{u} \gamma^\alpha (\not{p} - \not{k} + m) \gamma^\beta (\not{p} - \not{k} - \not{k}_1 + m) (\not{p} - \not{k} - \not{k}_1 + m) \gamma_\alpha (\not{p} - \not{k}_1 + m) \gamma_\beta u \\
N_{3e} &= \bar{u} \gamma^\alpha (\not{p} - \not{k} + m) \gamma^\beta (\not{p} - \not{k} - \not{k}_1 + m) \gamma_\alpha (\not{p} - \not{k}_1 + m) (\not{p} - \not{k}_1 + m) \gamma_\beta u
\end{aligned} \tag{47}$$

we see that the proof of equation (42) is tantamount to showing the equality of numerator factors to linear accuracy. IR power counting on the integral shows that we have to keep the terms in the numerator at most linear in the integration variables. To linear accuracy the first numerator pieces,  $N_1$  and  $N_{1c}$  are

$$\begin{aligned}
N_1 &= \bar{u} \gamma^\alpha (\not{p} + m) \gamma^0 (\not{p} + m) \gamma^\beta (\not{p} + m) \gamma_\alpha (\not{p} + m) \gamma_\beta u \\
&\quad - \bar{u} \gamma^\alpha \not{k} \gamma^0 (\not{p} + m) \gamma^\beta (\not{p} + m) \gamma_\alpha (\not{p} + m) \gamma_\beta u \\
&\quad - \bar{u} \gamma^\alpha (\not{p} + m) \gamma^0 \not{k} \gamma^\beta (\not{p} + m) \gamma_\alpha (\not{p} + m) \gamma_\beta u \\
&\quad - \bar{u} \gamma^\alpha (\not{p} + m) \gamma^0 (\not{p} + m) \gamma^\beta (\not{k} + \not{k}_1) \gamma_\alpha (\not{p} + m) \gamma_\beta u \\
&\quad - \bar{u} \gamma^\alpha (\not{p} + m) \gamma^0 (\not{p} + m) \gamma^\beta (\not{p} + m) \gamma_\alpha \not{k}_1 \gamma_\beta u
\end{aligned} \tag{48}$$

and

$$\begin{aligned}
N_{1c} &= \bar{u} \gamma^\alpha (\not{p} + m) (\not{p} + m) \gamma^\beta (\not{p} + m) \gamma_\alpha (\not{p} + m) \gamma_\beta u \\
&\quad - \bar{u} \gamma^\alpha \not{k} (\not{p} + m) \gamma^\beta (\not{p} + m) \gamma_\alpha (\not{p} + m) \gamma_\beta u \\
&\quad - \bar{u} \gamma^\alpha (\not{p} + m) \not{k} \gamma^\beta (\not{p} + m) \gamma_\alpha (\not{p} + m) \gamma_\beta u \\
&\quad - \bar{u} \gamma^\alpha (\not{p} + m) (\not{p} + m) \gamma^\beta (\not{k} + \not{k}_1) \gamma_\alpha (\not{p} + m) \gamma_\beta u \\
&\quad - \bar{u} \gamma^\alpha (\not{p} + m) (\not{p} + m) \gamma^\beta (\not{p} + m) \gamma_\alpha \not{k}_1 \gamma_\beta u
\end{aligned} \tag{49}$$

Note that the first terms in equations (48), (49) give the logarithmic infrared sensitive pieces, while the last 4 terms give the linear infrared sensitive parts. Comparing the first terms, it is easy to see the equality of the logarithmic pieces.

It is also straightforward to see that  $N_1|_{linear} = N_{1c}|_{linear}$ . The only difference in the numerators is the presence of the  $\gamma^0$  factor. Since the numerator is at most linear in  $k$  and  $k_1$ , either left or right to  $\gamma^0$  there will be only factors of  $(\not{p} + m)$  and  $\gamma$  matrices, which could be easily evaluated using the mass-shell condition. Then using that  $\gamma^0 u = u$  (since in rest frame) we have effectively replaced the  $\gamma^0$  by 1, which means the equality of the two numerator pieces. In the same way one can show that to linear accuracy  $N_2 = N_{2d}$  and  $N_3 = N_{3e}$ , thus the equality of numerators and hence equation (42) holds to linear accuracy. Therefore the logarithmic and linear infrared sensitive wave function renormalization pieces of the  $\Sigma_{22}$  group cancel

$$[9a) + 9b) + 9c) + 9d) + 9e)]_{wavefunction} = 0 \tag{50}$$

The cancellation of the logarithmic and linear wave function parts of group-4 can be shown in a similar way. The cancellation of logarithmic and linear wave function renormalization pieces in group-5 is discussed in the Appendix.

The first and third group do not cancel separately, since  $\Sigma_{21}$  contains a mass renormalization piece through its inner part,  $\Sigma_1$ . This piece will cancel with the corresponding mass

counterterm of  $\Sigma_{23}$ , and the sum of the two groups again cancel to the accuracy desired. To show the cancellation of the logarithmic and linear infrared sensitive pieces in the wave function renormalization, we again use the Ward-like identities in Figs 13a) and 13c).

At the two-loop level 1-particle reducible diagrams also contribute to the wave function renormalization. The relevant diagrams are shown in Fig. 14. The contribution of the diagrams (shown in the Figure) can be simply calculated using the perturbative expansion of  $Z^{1/2}$  (Eq. 32) multiplying each external line in the S-matrix element. As Fig. 14 shows, the wave function renormalization pieces from the two-loop order 1-particle reducible diagrams cancel.

#### IV. CANCELLATION OF THE INFRARED SENSITIVE TERMS ARISING FROM MASS RENORMALIZATION

Let us now consider the cancellation of the leading infrared sensitive piece (the one that is linearly divergent in the infrared) arising from the diagrams involving the mass renormalization of the heavy quark. As for the wave function case we begin with a discussion of the one loop case to exemplify our method and then the more complicated two loop example is considered.

##### A. Cancellation at One Loop

As discussed in the introduction, the pole mass of the heavy quark contains a long distance piece which is proportional linearly to an infrared cutoff, the first contribution starting at order  $\alpha$ . In fact, for our subsequent analysis it is convenient to separate out this piece and write for the pole mass to one loop order:

$$m_b = \bar{m} + b_1 g^2 \lambda \quad (51)$$

where, as before,  $\bar{m}$  is used to denote the short distance or the running mass, which itself is a power series expansion in  $g^2$ :

$$\bar{m} = m_0 + a_1 g^2. \quad (52)$$

We should emphasize our notation at this point. Even though one may use a gluon mass as an infrared cutoff at the one loop level, this is not a gauge invariant procedure beyond it. Thus  $\lambda$  refers to some gauge invariant cutoff. Throughout this paper, however we will not have any need to specify this infrared cutoff. Terms that are linearly divergent in the infrared are identified by power counting and cancellation of such terms is shown at the level of the corresponding Feynman integrands. Thus for example,

$$b_1 g^2 \lambda \equiv g^2 C_F \int_{linear} \frac{d^4 k}{(2\pi)^4} \frac{1}{k^2 + i\epsilon} \frac{1}{k_0 - i\epsilon}. \quad (53)$$

The various diagrams contributing to this order are shown in Fig. 6. Fig. 6a) is the bremsstrahlung contribution. To find the leading infrared sensitive contribution, we expand the leading effective hard vertex to first order in the offshellness, i.e.,

$$C(\not{p} - \not{k})^5 = C(\not{p} - \not{k} - m_b + m_b)^5 = C m_b^5 + C 5 m_b^4 (\not{p} - \not{k} - m_b) + \dots \quad (54)$$

This is an expansion of the leading effective vertex in  $(\not{p} - \not{k} - m_b)/m_b$  and it is understood that we keep such deviations from the mass shell in as much as they cancel the corresponding small denominators from the propagators. Then after this expansion, one of the fermion propagators in the integrand of the expression for Fig. 6 is cancelled (shown by a slash in the Figure) and we are left with an expression which resembles that for the self energy. In fact,

$$6a) = C 5 (\bar{m})^4 b_1 g^2 \lambda \bar{u} u \quad (55)$$

Next we have the contributions from the bremsstrahlung from the final state quark which as discussed earlier is replaced by the effective vertices for the gluon emission. The two diagrams with single gluon effective vertices of Figs. 6b) and 6c) give:

$$6b) + 6c) = 2 \times C(-i 5 m_b^4) \bar{u} (-i \Sigma_1(p)) u = -2 \times C 5 (\bar{m})^4 b_1 g^2 \lambda \bar{u} u. \quad (56)$$

Finally, in the lowest order diagram, Fig. 6d), we must express the leading effective vertex in terms of the short distance mass,

$$6d) = C m_b^5 = C(\bar{m} + b_1 g^2 \lambda)^5 = C \bar{m}^5 \bar{u} u + 5 C (\bar{m})^4 b_1 g^2 \lambda \bar{u} u. \quad (57)$$

Adding together all the order  $g^2$  terms we see the cancellation of the linearly infrared divergent pieces to this order when the decay rate is expressed in terms of the running mass  $\bar{m}$ . We next discuss the two loop example.

## B. Cancellation to Two Loops

As in the wave function renormalization, we group the two-loop 1 PI diagrams according to the five self-energy pieces shown in Fig. 7. These groups are now enlarged by new diagrams with the single and double gluon vertices (Fig. 3). Unlike in the wave function case, where each group of graphs cancelled separately, the cancellation of linear infrared sensitive pieces in the mass renormalization involves mixing between the different groups and mass shift terms from one loop graphs. This is essentially because whereas the wave function renormalization is multiplicative, the on-shell mass renormalization is additive.

By infrared power counting we can isolate the linear infrared sensitive pieces of the self-energy diagrams as

$$\begin{aligned} \Sigma_1|_{\not{p}=m_b} &= a_1 g^2 + b_1 g^2 \lambda \\ \Sigma_{2i}|_{\not{p}=m_b} &= a_{2i} g^4 + b_{2i} g^4 \lambda \quad i = 1 \dots 5 \end{aligned} \quad (58)$$

(Note that as before,  $\lambda$  denotes symbolically the linearly infrared sensitive pieces of the diagrams identified by power counting, not an actual infrared cutoff parameter.) Define the running mass as

$$\bar{m} = m_0 + a_1 g^2 + \sum_{i=1}^5 a_{2i} g^4. \quad (59)$$

Then the physical mass in terms of the running mass can be written as

$$m_b = \bar{m} + b_1 g^2 \lambda + \sum_{i=1}^5 b_{2i} g^4 \lambda. \quad (60)$$

### 1. Group-1 and Group-2

*a. Leading effective vertex and single gluon vertex graphs* The cancellation between the linear infrared sensitive pieces in the mass renormalization of the first two group of graphs with the corresponding single and double gluon vertex graphs is shown in Fig. 15. As before, the linear infrared sensitive pieces in the mass renormalization of the diagrams are identified by IR power counting, and will be referred simply as “linear mass pieces” or “linear pieces” of the diagrams in the following. Note that the cancellation involves the order  $g^4$  mass shift terms from the one-loop diagrams, as will be discussed below.

Let us first look at the first two graphs of Figs. 15, 15a) and 15b). The vertex of 15a) is proportional to  $(\not{p} - \not{k})^5$  (we will always take  $k$  the momentum of the first outgoing gluon). As discussed for the 1-loop case, the linear mass pieces of the graphs are extracted by expanding the vertex around mass shell up to linear terms in the integration variables, identified by power counting. In the case of 15a)

$$C (\not{p} - \not{k})^5 \Big|_{\text{mass, linear}} = C 5 m_b^4 (\not{p} - \not{k} - m_b) + C 10 m_b^3 (\not{p} - \not{k} - m_b)^2 \quad (61)$$

The first term in the vertex expansion,  $C m_b^5$ , gives the wave function renormalization piece of the diagram. The remaining terms in the vertex expansion contribute to the mass renormalization parts of the diagram. These are at least linear in the offshellness  $(\not{p} - \not{k} - m_b)$ , canceling a propagator of the graph with an extra factor of  $i$  left. This cancellation is as was mentioned earlier for the one loop case denoted by a slash on the corresponding propagator in the figures.

The vertex of 15b) is a single gluon vertex (Fig. 3), its expansion up to terms giving linear infrared sensitivity in the integration

$$\begin{aligned} [vertex]_{\alpha}^a \Big|_{\text{linear}} &= C g m_b^4 T^a \left[ (\not{p} - \not{k})^4 \gamma_{\alpha} + (\not{p} - \not{k})^3 \gamma_{\alpha} (\not{p} - \not{k} - \not{k}_1) + \right. \\ &\left. \cdots + \gamma_{\alpha} (\not{p} - \not{k} - \not{k}_1)^4 \right] \Big|_{\text{linear}} = C \frac{5}{i} m_b^4 T^a i g \gamma_{\alpha} + C \frac{10}{i} m_b^3 T^a (\not{p} - \not{k} - m_b) i g \gamma_{\alpha} \end{aligned} \quad (62)$$

Substituting the linearized expressions for the vertices, we find that 15a) and 15b) cancel. The same type of cancellation applies for the next pair of graphs, 15c) and 15d)

$$15a) + 15b) = 0 \quad 15c) + 15d) = 0. \quad (63)$$

The case of 15e-f) and 15g-h) is a little more complicated. The leading effective vertex is expanded the same way as in (61), giving

$$\begin{aligned} 15e) &= C 5 i m_b^4 (-i \Sigma_{22}) \Big|_{\not{p}=m_b} \bar{u} u - C 10 m_b^3 \left( C_F^2 - \frac{C_F C_A}{2} \right) \bar{u} i g \gamma^{\alpha} i g \gamma^{\beta} \times \\ &\int d^4 k d^4 k_1 \frac{i}{\not{p} - \not{k} - \not{k}_1 - m} i g \gamma_{\alpha} \frac{i}{\not{p} - \not{k}_1 - m} i g \gamma_{\beta} \frac{-i - i}{k^2 k_1^2} u \end{aligned} \quad (64)$$



Here however the expansion of the single gluon vertex to linear IR sensitive terms in the integration results in 3 terms:

$$\begin{aligned}
[vertex]_\beta^b|_{linear} &= CgT^b \left[ (\not{p} - \not{k})^4 \gamma_\beta + (\not{p} - \not{k})^3 \gamma_\beta (\not{p} - \not{k} - \not{k}_1) + \dots + \right. \\
&\quad \left. \gamma_\beta (\not{p} - \not{k} - \not{k}_1)^4 \right] |_{linear} = C \frac{5}{i} m_b^4 ig \gamma_\beta T^b + C \frac{10}{i} m_b^3 (\not{p} - \not{k} - m_b) ig \gamma_\beta T^b \\
&\quad + C \frac{10}{i} m_b^3 ig \gamma_\beta T^b (\not{p} - \not{k} - \not{k}_1 - m_b)
\end{aligned} \tag{65}$$

From (64) we get for 15f)

$$\begin{aligned}
15f) &= -C5im_b^4 (-i\Sigma_{22})|_{\not{p}=m_b} \bar{u}u + C10m_b^3 \left( C_F^2 - \frac{C_F C_A}{2} \right) \bar{u} ig \gamma^\alpha ig \gamma^\beta \times \\
&\quad \int d^4k d^4k_1 \frac{i}{\not{p} - \not{k} - \not{k}_1 - m} ig \gamma_\alpha \frac{i}{\not{p} - \not{k}_1 - m} ig \gamma_\beta \frac{-i}{k^2} \frac{-i}{k_1^2} u + \\
&\quad C10m_b^3 \left( C_F^2 - \frac{C_F C_A}{2} \right) \bar{u} ig \gamma^\alpha \int d^4k d^4k_1 \frac{i}{\not{p} - \not{k} - m} \times \\
&\quad ig \gamma^\beta ig \gamma_\alpha \frac{i}{\not{p} - \not{k}_1 - m} ig \gamma_\beta \frac{-i}{k^2} \frac{-i}{k_1^2} u
\end{aligned} \tag{66}$$

Unlike the first two pairs of graphs, 15e) and 15f) do not cancel. The sum of the two graphs is the last term of 15f). Calculating for 15g) and 15h) in the same way, we find that

$$\begin{aligned}
15g) + 15h) &= 15e) + 15f) \\
15e) + 15f) + 15g) + 15h) &= 2 \times C10m_b^3 \left( C_F^2 - \frac{C_F C_A}{2} \right) \bar{u} ig \gamma^\alpha \times \\
&\quad \int d^4k d^4k_1 \frac{i}{\not{p} - \not{k} - m} ig \gamma^\beta ig \gamma_\alpha \frac{i}{\not{p} - \not{k}_1 - m} ig \gamma_\beta \frac{-i}{k^2} \frac{-i}{k_1^2} u
\end{aligned} \tag{67}$$

Next consider the diagrams 15i)-l). Expanding the vertices around mass shell and keeping linear infrared sensitive terms in the integration gives

$$15i) = C5im_b^4 (-i\Sigma_{21})|_{\not{p}=m_b} \bar{u}u \tag{68}$$

(Note that further expansion of the leading effective vertex would give a quadratically infrared sensitive piece by IR power counting.)

The single gluon vertex of 15j) is expanded to linear accuracy as

$$\begin{aligned}
[vertex]_\alpha^a|_{linear} &= CgT^a \left[ \not{p}^4 \gamma_\alpha + \not{p}^3 \gamma_\alpha (\not{p} - \not{k}) + \dots + \gamma_\alpha (\not{p} - \not{k})^4 \right] |_{linear} = \\
&\quad C \frac{5}{i} m_b^4 T^a ig \gamma_\alpha + C \frac{10}{i} m_b^3 T^a ig \gamma_\alpha (\not{p} - \not{k} - m_b)
\end{aligned} \tag{69}$$

Substituting the vertex expansion (69), 15j) becomes

$$\begin{aligned}
15j) &= -C5im_b^4 (-i\Sigma_{21})|_{\not{p}=m_b} \bar{u}u \\
&\quad + C10m_b^3 C_F^2 \bar{u} ig \gamma^\alpha ig \gamma^\beta \int d^4k d^4k_1 \frac{i}{\not{p} - \not{k} - \not{k}_1 - m} ig \gamma_\beta \frac{i}{\not{p} - \not{k} - m} ig \gamma_\alpha \frac{-i}{k^2} \frac{-i}{k_1^2} u
\end{aligned} \tag{70}$$

A similar calculation for 15k) gives

$$15k) = -C5im_b^4(-i\Sigma_{21})\Big|_{p=m_b} \bar{u}u \quad (71)$$

$$+C10m_b^3C_F^2\bar{u}ig\gamma^\alpha\int d^4kd^4k_1\frac{i}{\not{p}-\not{k}-m}ig\gamma^\beta\frac{i}{\not{p}-\not{k}-\not{k}_1-m}ig\gamma_\beta ig\gamma_\alpha\frac{-i}{k^2}\frac{-i}{k_1^2}u$$

Diagram 15l) is the mass shift term of the tree level amplitude corresponding to  $\Sigma_{21}$

$$15l) = C\bar{u}\not{p}^5u\Big|_{\Sigma_{21}} = Cm_b^5\Big|_{\Sigma_{21}} \bar{u}u = C5\bar{m}^4g^4b_{21}\lambda\bar{u}u \quad (72)$$

Adding the 4 graphs and using that  $\Sigma_{21} = a_{21} + b_{21}g^4\lambda$  we arrive at

$$15i) + 15j) + 15k) + 15l) = \quad (73)$$

$$C10m_b^3C_F^2\bar{u}ig\gamma^\alpha ig\gamma^\beta\int d^4kd^4k_1\frac{i}{\not{p}-\not{k}-\not{k}_1-m}ig\gamma_\beta\frac{i}{\not{p}-\not{k}-m}ig\gamma_\alpha\frac{-i}{k^2}\frac{-i}{k_1^2}u +$$

$$C10m_b^3C_F^2\bar{u}ig\gamma^\alpha\int d^4kd^4k_1\frac{i}{\not{p}-\not{k}-m}ig\gamma^\beta\frac{i}{\not{p}-\not{k}-\not{k}_1-m}ig\gamma_\beta ig\gamma_\alpha\frac{-i}{k^2}\frac{-i}{k_1^2}u$$

The calculation for the next 4 graphs, 15m-p) is similar to 15i-l. Note however that in the leading effective vertex expansion of 15m) we must keep the first 2 terms, unlike in the case of 15i), resulting in an extra term. Apart from this, the difference is only in the gamma matrix and color structure. For the sum we find

$$15m) + 15n) + 15o) + 15p) = \quad (74)$$

$$-C10m_b^3\left(C_F^2 - \frac{C_FC_A}{2}\right)\bar{u}ig\gamma^\alpha \times$$

$$\int d^4kd^4k_1\frac{i}{\not{p}-\not{k}-m}ig\gamma_\beta ig\gamma_\alpha\frac{i}{\not{p}-\not{k}_1-m}ig\gamma^\beta\frac{-i}{k^2}\frac{-i}{k_1^2}u$$

$$+C10m_b^3\left(C_F^2 - \frac{C_FC_A}{2}\right)\bar{u}ig\gamma^\alpha \times$$

$$\int d^4kd^4k_1\frac{i}{\not{p}-\not{k}-m}ig\gamma^\beta\frac{i}{\not{p}-\not{k}-\not{k}_1-m}ig\gamma_\alpha ig\gamma_\beta\frac{-i}{k^2}\frac{-i}{k_1^2}u$$

$$+C10m_b^3\left(C_F^2 - \frac{C_FC_A}{2}\right)\bar{u}ig\gamma^\alpha ig\gamma^\beta \times$$

$$\int d^4kd^4k_1\frac{i}{\not{p}-\not{k}-\not{k}_1-m}ig\gamma_\alpha\frac{i}{\not{p}-\not{k}_1-m}ig\gamma_\beta\frac{-i}{k^2}\frac{-i}{k_1^2}u$$

Summarizing the leading and single gluon effective vertex diagrams contribute with

$$15a) + \dots + 15p) = \quad (75)$$

$$C10m_b^3\left\{C_F^2\bar{u}ig\gamma^\alpha ig\gamma^\beta\int d^4kd^4k_1\frac{i}{\not{p}-\not{k}-\not{k}_1-m}ig\gamma_\beta\frac{i}{\not{p}-\not{k}-m}ig\gamma_\alpha\frac{-i}{k^2}\frac{-i}{k_1^2}u\right.$$

$$+\left(C_F^2 - \frac{C_FC_A}{2}\right)\bar{u}ig\gamma^\alpha ig\gamma^\beta\int d^4kd^4k_1\frac{i}{\not{p}-\not{k}-\not{k}_1-m}ig\gamma_\alpha\frac{i}{\not{p}-\not{k}_1-m}ig\gamma_\beta\frac{-i}{k^2}\frac{-i}{k_1^2}u$$

$$+C_F^2\bar{u}ig\gamma^\alpha\int d^4kd^4k_1\frac{i}{\not{p}-\not{k}-m}ig\gamma^\beta\frac{i}{\not{p}-\not{k}-\not{k}_1-m}ig\gamma_\beta ig\gamma_\alpha\frac{-i}{k^2}\frac{-i}{k_1^2}u$$

$$\begin{aligned}
& + \left( C_F^2 - \frac{C_F C_A}{2} \right) \bar{u} i g \gamma^\alpha \int d^4 k d^4 k_1 \frac{i}{\not{p} - \not{k} - m} i g \gamma^\beta \frac{i}{\not{p} - \not{k} - \not{k}_1 - m} i g \gamma_\alpha i g \gamma_\beta \frac{-i}{k^2} \frac{-i}{k_1^2} u \\
& + \left( C_F^2 - \frac{C_F C_A}{2} \right) \bar{u} i g \gamma^\alpha \int d^4 k d^4 k_1 \frac{i}{\not{p} - \not{k} - m} i g \gamma_\beta i g \gamma_\alpha \frac{i}{\not{p} - \not{k}_1 - m} i g \gamma^\beta \frac{-i}{k^2} \frac{-i}{k_1^2} u \Big\}
\end{aligned}$$

*b. Double vertex graphs* Since we keep infrared sensitive terms to linear accuracy, power counting shows that the double gluon vertex need not be expanded any further, and so it is simplified to

$$[double\ vertex]_{\alpha,\beta}^{a,b} = C 10 g^2 m_b^3 \left( \gamma_\alpha \gamma_\beta T^a T^b + \gamma_\beta \gamma_\alpha T^b T^a \right) \quad (76)$$

From the above,

$$\begin{aligned}
15r) = & -C 10 m_b^3 C_F^2 \bar{u} i g \gamma^\beta i g \gamma^\alpha \times \\
& \int d^4 k d^4 k_1 \frac{i}{\not{p} - \not{k} - \not{k}_1 - m} i g \gamma_\alpha \frac{i}{\not{p} - \not{k}_1 - m} i g \gamma_\beta \frac{-i}{k^2} \frac{-i}{k_1^2} u \\
& -C 10 m_b^3 \left( C_F^2 - \frac{C_F C_A}{2} \right) \bar{u} i g \gamma^\alpha i g \gamma^\beta \times \\
& \int d^4 k d^4 k_1 \frac{i}{\not{p} - \not{k} - \not{k}_1 - m} i g \gamma_\alpha \frac{i}{\not{p} - \not{k}_1 - m} i g \gamma_\beta \frac{-i}{k^2} \frac{-i}{k_1^2} u
\end{aligned} \quad (77)$$

$$\begin{aligned}
15s) = & -C 10 m_b^3 C_F^2 \bar{u} i g \gamma^\alpha \times \\
& \int d^4 k d^4 k_1 \frac{i}{\not{p} - \not{k} - m} i g \gamma^\beta \frac{i}{\not{p} - \not{k} - \not{k}_1 - m} i g \gamma_\beta i g \gamma_\alpha \frac{-i}{k^2} \frac{-i}{k_1^2} u \\
& -C 10 m_b^3 \left( C_F^2 - \frac{C_F C_A}{2} \right) \bar{u} i g \gamma^\alpha \times \\
& \int d^4 k d^4 k_1 \frac{i}{\not{p} - \not{k} - m} i g \gamma^\beta \frac{i}{\not{p} - \not{k} - \not{k}_1 - m} i g \gamma_\alpha i g \gamma_\beta \frac{-i}{k^2} \frac{-i}{k_1^2} u
\end{aligned} \quad (78)$$

$$\begin{aligned}
15t) = & -C 10 m_b^3 C_F^2 \bar{u} i g \gamma^\alpha \times \\
& \int d^4 k d^4 k_1 \frac{i}{\not{p} - \not{k} - m} i g \gamma_\alpha i g \gamma_\beta \frac{i}{\not{p} - \not{k}_1 - m} i g \gamma^\beta \frac{-i}{k^2} \frac{-i}{k_1^2} u \\
& -C 10 m_b^3 \left( C_F^2 - \frac{C_F C_A}{2} \right) \bar{u} i g \gamma^\alpha \times \\
& \int d^4 k d^4 k_1 \frac{i}{\not{p} - \not{k} - m} i g \gamma_\beta i g \gamma_\alpha \frac{i}{\not{p} - \not{k}_1 - m} i g \gamma^\beta \frac{-i}{k^2} \frac{-i}{k_1^2} u
\end{aligned} \quad (79)$$

The sum of the linear infrared sensitive pieces of the double vertex graphs is therefore

$$\begin{aligned}
& 15r) + 15s) + 15t) = \\
& -C 10 m_b^3 \left\{ C_F^2 \bar{u} i g \gamma^\beta i g \gamma^\alpha \int d^4 k d^4 k_1 \frac{i}{\not{p} - \not{k} - \not{k}_1 - m} i g \gamma_\alpha \frac{i}{\not{p} - \not{k}_1 - m} i g \gamma_\beta \frac{-i}{k^2} \frac{-i}{k_1^2} u \right. \\
& \left. + \left( C_F^2 - \frac{C_F C_A}{2} \right) \bar{u} i g \gamma^\alpha i g \gamma^\beta \int d^4 k d^4 k_1 \frac{i}{\not{p} - \not{k} - \not{k}_1 - m} i g \gamma_\alpha \frac{i}{\not{p} - \not{k}_1 - m} i g \gamma_\beta \frac{-i}{k^2} \frac{-i}{k_1^2} u \right.
\end{aligned} \quad (80)$$

$$\begin{aligned}
& + C_F^2 \bar{u} i g \gamma^\alpha \int d^4 k d^4 k_1 \frac{i}{\not{p} - \not{k} - m} i g \gamma^\beta \frac{i}{\not{p} - \not{k} - \not{k}_1 - m} i g \gamma_\beta i g \gamma_\alpha \frac{-i}{k^2} \frac{-i}{k_1^2} u \\
& + \left( C_F^2 - \frac{C_F C_A}{2} \right) \bar{u} i g \gamma^\alpha \int d^4 k d^4 k_1 \frac{i}{\not{p} - \not{k} - m} i g \gamma^\beta \frac{i}{\not{p} - \not{k} - \not{k}_1 - m} i g \gamma_\alpha i g \gamma_\beta \frac{-i}{k^2} \frac{-i}{k_1^2} u \\
& + C_F^2 \bar{u} i g \gamma^\alpha \int d^4 k d^4 k_1 \frac{i}{\not{p} - \not{k} - m} i g \gamma_\alpha i g \gamma_\beta \frac{i}{\not{p} - \not{k}_1 - m} i g \gamma^\beta \frac{-i}{k^2} \frac{-i}{k_1^2} u \\
& + \left( C_F^2 - \frac{C_F C_A}{2} \right) \bar{u} i g \gamma^\alpha \int d^4 k d^4 k_1 \frac{i}{\not{p} - \not{k} - m} i g \gamma_\beta i g \gamma_\alpha \frac{i}{\not{p} - \not{k}_1 - m} i g \gamma^\beta \frac{-i}{k^2} \frac{-i}{k_1^2} u \Big\}
\end{aligned}$$

Adding (75) and (80) the sum of the leading, single, and double gluon effective vertex diagrams gives

$$\begin{aligned}
15a) + \dots + 15t) = & \\
& -C10m_b^3 C_F^2 \bar{u} i g \gamma^\alpha \int d^4 k d^4 k_1 \frac{i}{\not{p} - \not{k} - m} i g \gamma_\alpha i g \gamma_\beta \frac{i}{\not{p} - \not{k}_1 - m} i g \gamma^\beta \frac{-i}{k^2} \frac{-i}{k_1^2} u = \\
& -C10m_b^3 (-i\Sigma_1|_{\not{p}=m_b})^2 \bar{u} u
\end{aligned} \tag{81}$$

Using power counting, the linear term of the sum is (with the use of equation (58))

$$15a) + \dots + 15t) = C20\bar{m}^3 a_1 b_1 g^4 \lambda \bar{u} u \tag{82}$$

*c. Mass-shift terms from 1-loop graphs* The 1-loop diagrams (Fig. 6) also contribute to the order  $g^4$  cancellations via their mass shift terms. Using the results of section IV A, the linear mass renormalization pieces of the 1-loop graphs to order  $g^4$  are

$$\begin{aligned}
6a) + 6b) + 6c) = & -C5m_b^4 \Sigma|_{\not{p}=m_b} \bar{u} u \Big|_{linear} \\
= & -C5 \left( \bar{m} + a_1 g^2 + b_1 g^2 \lambda \right)^4 \left( a_1 g^2 + b_1 g^2 \lambda \right) \bar{u} u \Big|_{linear} \\
= & -C5\bar{m}^4 b_1 g^2 \lambda \bar{u} u - C40\bar{m}^3 a_1 b_1 g^4 \lambda \bar{u} u
\end{aligned} \tag{83}$$

$$\begin{aligned}
6d) = & C m_b^5 \bar{u} u \Big|_{linear} = C \left( \bar{m} + a_1 g^2 + b_1 g^2 \lambda + \sum_{i=1}^4 a_{2i} g^4 + \sum_{i=1}^4 b_{2i} g^4 \lambda \right)^5 \bar{u} u \Big|_{linear} \\
= & C5\bar{m}^4 b_1 g^2 \lambda \bar{u} u + C5\bar{m}^4 \sum_{i=1}^4 b_{2i} g^4 \lambda \bar{u} u + C20\bar{m}^3 a_1 b_1 g^4 \lambda \bar{u} u
\end{aligned} \tag{84}$$

As we have shown before, the order  $g^2$  terms of the 1-loop diagrams cancel. The mass shift terms due to the order  $g^4$  self-energy corrections were already included in the calculation. The order  $g^4$  terms we have not included so far are the “cross terms”, those proportional to  $a_1 b_1$ . These are the terms we denoted with the expression “mass shift terms” on Fig. 15x), summing up to

$$15x) = -C20\bar{m}^3 a_1 b_1 g^4 \lambda \bar{u} u \tag{85}$$

This contribution cancels the remaining linear term of the 2-loop vertex diagrams of group-1 and group-2, (82), so the linear infrared sensitive terms in the mass renormalization of the first two group of diagrams with the mass shift terms from the 1-loop diagrams cancel

$$15a) + \dots + 15x) = 0. \tag{86}$$

## 2. Group-3 and the group of 1-particle reducible diagrams

The linear mass renormalization parts of the group-3 diagrams cancel with the corresponding pieces of 1-particle reducible graphs, as shown in Fig. 16.

Expanding the leading effective vertex of 16a) as in (61), and the single gluon vertex of 16b) as in (69) to linear accuracy it is easy to see that 16a) and 16b) cancel. The next two pair of graphs 16c) and 16d) cancel similarly:

$$16a) + 16b) = 0 \quad 16c) + 16d) = 0 \quad (87)$$

The mass shift term of the tree amplitude, corresponding to  $\Sigma_{23}$ , 16g)

$$16g) = C m_b^5 \Big|_{\Sigma_{23}} \bar{u}u = 5\bar{m}^4 b_{23} g^4 \lambda \bar{u}u \quad (88)$$

cancel with the remainder of the one-particle reducible group, as we will show below. For the 1-particle reducible diagrams the leading effective vertex of 16e), 16f) and the corresponding mass counterterm graphs is expanded to first order in the offshellness

$$(\not{p} - \not{k})^5 \Big|_{mass, linear} = C 5 m_b^4 (\not{p} - \not{k} - m_b) \quad (89)$$

Keeping the second term as in (61) would result in a quadratic infrared sensitive term by IR power counting. From the vertex expansion (89) we get for the linear mass pieces of the diagrams

$$16e) + 16f) + \dots = -C 5 i m_b^4 \left( Z^{-1} - 1 \right)_{g^2} (-i \Sigma_1) \Big|_{\not{p}=m_b} \bar{u}u \quad (90)$$

The ellipsis in the formula denote the inclusion of the mass counterterm diagrams, as in Fig. 16. Here we used the one-loop Ward-like identity (Fig. 5) and the perturbative expansion of  $Z^{1/2}$ , Eq. (32).

For the remaining one-particle reducible diagrams 16h-k) the expansion of the single gluon vertex up to linear infrared sensitive terms in the integration gives one term

$$[vertex]_\alpha^a \Big|_{linear} = C \frac{5}{i} m_b^4 i g \gamma_\alpha T^a \quad (91)$$

Substituting the vertex expansion (91), we find that

$$16h) + 16i) + \dots = 16j) + 16k) + \dots = C 5 i m_b^4 \left( Z^{-1} - 1 \right)_{g^2} (-i \Sigma_1) \Big|_{\not{p}=m_b} \bar{u}u. \quad (92)$$

Thus the sum of the linear pieces of the 1-particle reducible graphs is

$$\begin{aligned} 16e) + \dots 16k) + \dots &= C 5 i m_b^4 \left( Z^{-1} - 1 \right)_{g^2} (-i \Sigma_1) \Big|_{\not{p}=m_b, linear} \bar{u}u \\ &= C 5 \bar{m}^4 \left( Z^{-1} - 1 \right)_{g^2} b_1 g^2 \lambda \bar{u}u \end{aligned} \quad (93)$$

The sum (93) cancels the leftover  $\Sigma_{23}$  mass shift piece, (88), since by the one loop Ward-like identity (Fig. 5)

$$b_{23}g^2 = -b_1 \left( Z^{-1} - 1 \right)_{g^2} \quad (94)$$

and Eq. (88) (Fig. 16g)) becomes

$$16g) = C5\bar{m}^4 b_{23}g^4 \lambda \bar{u}u = -C5\bar{m}^4 b_1 g^2 \left( Z^{-1} - 1 \right)_{g^2} \lambda \bar{u}u, \quad (95)$$

Hence all linear mass renormalization pieces of the group-3 and the 1-particle reducible diagrams cancel:

$$16g) + 16e) + \cdots 16k) + \cdots = 0 \quad (96)$$

### 3. Group-4

The cancellation within group-4 (Fig. 17) proceeds in the same way as for the 1-loop diagrams (see Fig. 6, and section IV A).

### 4. Group-5

Fig. 18 shows the cancellation between the group-5 diagrams. We can calculate the linear parts of the first 4 diagrams 18a-d) expanding the leading effective vertex to second order and the single gluon vertex to first order in the offshellness. A straightforward calculation gives

$$18a) + 18b) = 0 \quad 18c) + 18d) = 0 \quad (97)$$

The case of the next 4 diagrams, 18e-h) is more interesting. 18e), the mass-shift piece of the tree amplitude corresponding to  $\Sigma_{25}$  is

$$18e) = C m_b^5 \Big|_{\Sigma_{25}} \bar{u}u = 5C\bar{m}^4 b_{25}g^4 \lambda \bar{u}u \quad (98)$$

Denoting the triple gluon vertex with  $S_{\alpha\beta\delta}^{abc}$ , the next diagram, 18f) gives

$$\begin{aligned} 18f) &= \bar{u}ig\gamma^\alpha T^a \int d^4k_b d^4k_c \frac{i}{\not{p} - \not{k}_b - \not{k}_c - m} \times \\ &[vertex]^{\beta,b} \frac{i}{\not{p} - \not{k}_c - m} ig\gamma^\delta T^c S_{\alpha\beta\delta}^{abc} \frac{-i}{k_b^2} \frac{-i}{k_c^2} \frac{-i}{(k_b + k_c)^2} \\ S_{\alpha\beta\delta}^{abc} &= gf^{abc} \left[ g_{\alpha\beta} (k_a - k_b)_\delta + g_{\beta\delta} (k_b - k_c)_\alpha + g_{\delta\alpha} (k_c - k_a)_\beta \right] \end{aligned} \quad (99)$$

The single gluon vertex is expanded to linear accuracy as follows:

$$\begin{aligned} [vertex]^{\beta,b} \Big|_{linear} &= C \frac{5}{i} m_b^4 ig\gamma^\beta T^b + C \frac{10}{i} m_b^3 (\not{p} - \not{k}_b - \not{k}_c - m_b) ig\gamma^\beta T^b \\ &+ C \frac{10}{i} m_b^3 ig\gamma^\beta T^b (\not{p} - \not{k}_c - m_b) \end{aligned} \quad (100)$$

Substituting the linearized vertex, 18f) gives 3 terms

$$\begin{aligned}
18f) = & -C5im_b^4 (-i\Sigma_{25})|_{\not{p}=m_b} \bar{u}u + C10m_b^3 \bar{u}ig\gamma^\alpha T^a ig\gamma^\beta T^b \times \\
& \int d^4k_b d^4k_c \frac{i}{\not{p} - \not{k}_c - m} ig\gamma^\delta T^c S_{\alpha\beta\delta}^{abc} \frac{-i-i}{k_b^2} \frac{-i}{k_c^2} \frac{-i}{(k_b+k_c)^2} u + \\
& C10m_b^3 \bar{u}ig\gamma^\alpha T^a \int d^4k_b d^4k_c \frac{i}{\not{p} - \not{k}_b - \not{k}_c - m} ig\gamma^\beta T^b ig\gamma^\delta T^c S_{\alpha\beta\delta}^{abc} \frac{-i-i}{k_b^2} \frac{-i}{k_c^2} \frac{-i}{(k_b+k_c)^2} u
\end{aligned} \tag{101}$$

To get the linear terms of 18g) and 18h), we need to keep only the first term in the expansion of the double gluon vertex. Thus

$$\begin{aligned}
18g) = & C10m_b^3 g^2 \bar{u} [\gamma^\alpha \gamma^\beta T^a T^b + \gamma^\beta \gamma^\alpha T^b T^a] \times \\
& \int d^4k_b d^4k_c \frac{i}{\not{p} - \not{k}_c - m} ig\gamma^\delta T^c S_{\alpha\beta\delta}^{abc} \frac{-i-i}{k_b^2} \frac{-i}{k_c^2} \frac{-i}{(k_b+k_c)^2} u
\end{aligned} \tag{102}$$

and

$$\begin{aligned}
18h) = & C10m_b^3 g^2 \bar{u}ig\gamma^\alpha T^a \times \\
& \int d^4k_b d^4k_c \frac{i}{\not{p} - \not{k}_b - \not{k}_c - m} [\gamma^\beta \gamma^\delta T^b T^c + \gamma^\delta \gamma^\beta T^c T^b] S_{\alpha\beta\delta}^{abc} \frac{-i-i}{k_b^2} \frac{-i}{k_c^2} \frac{-i}{(k_b+k_c)^2} u
\end{aligned} \tag{103}$$

Using that  $\Sigma_{25} = a_{25}g^4 + b_{25}g^4\lambda$ , the sum of the group-5 graphs gives

$$\begin{aligned}
18a) + \dots + 18h) = & \\
& -C10m_b^3 \bar{u}ig\gamma^\alpha T^a \int d^4k_b d^4k_c \frac{i}{\not{p} - \not{k}_b - \not{k}_c - m} ig\gamma^\delta T^c ig\gamma^\beta T^b S_{\alpha\beta\delta}^{abc} \frac{-i-i}{k_b^2} \frac{-i}{k_c^2} \frac{-i}{(k_b+k_c)^2} u \\
& -C10m_b^3 \bar{u}ig\gamma^\beta T^b ig\gamma^\alpha T^a \int d^4k_b d^4k_c \frac{i}{\not{p} - \not{k}_c - m} ig\gamma^\delta T^c S_{\alpha\beta\delta}^{abc} \frac{-i-i}{k_b^2} \frac{-i}{k_c^2} \frac{-i}{(k_b+k_c)^2} u
\end{aligned} \tag{104}$$

This remainder can be shown to be zero (up to linear accuracy) by renaming variables for example in the first integral for  $k'_c = (k_b + k_c)$  and  $k'_b = -k_c$ . Therefore the linear mass renormalization pieces of group-5 diagrams cancel.

## V. SUMMARY AND CONCLUSIONS.

In this paper we have shown by explicit perturbative calculations upto the second loop order, that when the inclusive decay width of a heavy quark is expressed in terms of the short distance mass, there is complete accord with the operator product expansion and the leading power corrections are of order  $1/m_b^2$ . This is the first such calculation to the second loop order that checks the dependence on the infrared cutoff to linear accuracy for the non-abelian theory. Because of the non-abelian interactions there could have been potential problems due to the singularity in the  $t$  channel for processes involving the forward scattering of soft gluons. However we see explicitly that these do not hinder the cancellation of the infrared sensitive terms to linear accuracy.

As emphasized earlier, the above result is true not just for the semileptonic decay considered in this paper but for any inclusive decay, like for example the radiative one. Such

a cancellation was linked to the KLN theorem which had been suggested earlier [7] to be the general principle behind this for inclusive enough observables. Since for the inclusive decay, there is only a single particle in the initial state, our calculations enjoyed several simplifications. It is known [10] that for at least two colored particles in the initial state there is a breakdown of the Bloch Nordsieck mechanism in perturbation theory. Thus it would be interesting to investigate the fate of the  $1/Q$  corrections for the Drell Yan process. For this process the initial state is no longer trivial and in addition further new complications arise in higher loops due to the mixing of soft and collinear singularities [11]. The  $1/Q$  corrections are known [12] to cancel to one loop order and the situation at higher loops is an open question. The techniques developed in this paper would be useful for this study as well, and we hope to return to this question in a future publication.

## VI. ACKNOWLEDGEMENTS

This work was supported in part by the US Department of Energy.

### APPENDIX A: CANCELLATION OF INFRARED SENSITIVE TERMS TO LINEAR ACCURACY IN THE WAVE FUNCTION RENORMALIZATION: GROUP-5

For the last group of diagrams (Fig. 12) the presence of the non-abelian vertex makes the algebra a little more complicated. The calculation proceeds essentially along the same lines as for the second group of diagrams (see section III B). We would like to show that for the logarithmically and linearly infrared sensitive parts (referred to as “logarithmic and linear pieces” in the following) of the diagrams of Fig. 12

$$\begin{aligned} [12a) + 12b)]_{\text{wavefunction}} &= -Cm_b^5 (Z^{-1} - 1)_{g^4, \Sigma_{25}} \bar{u}u \\ &= -[12c) + 12d)]_{\text{wavefunction}} \end{aligned} \quad (\text{A1})$$

As before, the logarithmically and linearly infrared sensitive pieces of the integrals are isolated by IR power counting. In the rest frame of the heavy quark  $p = (m_b, 0, 0, 0)$ , and

$$(Z^{-1} - 1)_{g^4, \Sigma_{25}} = -\frac{\bar{u} \frac{\partial \Sigma_{25}}{\partial p_\nu} \Big|_{\not{p}=m_b} u}{\bar{u} \gamma^\nu u} = -\frac{\bar{u} \frac{\partial \Sigma_{25}}{\partial p_0} \Big|_{\not{p}=m_b} u}{\bar{u} u} \quad (\text{A2})$$

so we would like to show that for the logarithmic and linear terms in the integration

$$Cm_b^5 \bar{u} \frac{\partial \Sigma_{25}}{\partial p_0} \Big|_{\not{p}=m_b} u = iCm_b^5 \bar{u} \frac{\partial(-i\Sigma_{25})}{\partial p_0} \Big|_{\not{p}=m_b} u = -[12c) + 12d)]_{\text{wavefunction}} \quad (\text{A3})$$

As before, the derivation of  $\Sigma_{25}$  with respect to  $p_0$  results in an insertion of an extra vertex  $i\gamma^0$  and an extra propagator in all possible way. The resulting diagrams are similar to 12c) and 12d) with the  $Cm_b^5$  vertex replaced by  $-Cm_b^5 \gamma^0$  (shown in Fig. 13). Writing out explicitly



$$\begin{aligned}
Cm_b^5 \bar{u} \frac{\partial \Sigma_{25}}{\partial p_0} \Big|_{\not{p}=m_b} u &= -Cm_b^5 \frac{C_F C_A}{2} (ig)^4 \times \left\{ \int d^4 k_b d^4 k_c N_1 \times \right. \\
&\left[ \frac{i}{-2p(k_b + k_c) + (k_b + k_c)^2} \right]^2 \frac{i}{-2pk_c + k_c^2} \frac{-i-i}{k_c^2} \frac{-i}{k_b^2} \frac{-i}{(k_b + k_c)^2} + \int d^4 k_b d^4 k_c N_2 \times \\
&\left. \frac{i}{-2p(k_b + k_c) + (k_b + k_c)^2} \left[ \frac{i}{-2pk_c + k_c^2} \right]^2 \frac{-i-i}{k_c^2} \frac{-i}{k_b^2} \frac{-i}{(k_b + k_c)^2} \right\}
\end{aligned} \tag{A4}$$

Denoting the triple gluon vertex by  $S_{\alpha\beta\delta}$  (where the color factor and the coupling are taken out) and  $k_a = -(k_b + k_c)$

$$\begin{aligned}
N_1 &= \bar{u} \gamma^\alpha (\not{p} + \not{k}_a + m) \gamma^0 (\not{p} + \not{k}_a + m) \gamma^\beta (\not{p} - \not{k}_c + m) \gamma^\delta S_{\alpha\beta\delta} u \\
N_2 &= \bar{u} \gamma^\alpha (\not{p} + \not{k}_a + m) \gamma^\beta (\not{p} - \not{k}_c + m) \gamma^0 (\not{p} - \not{k}_c + m) \gamma^\delta S_{\alpha\beta\delta} u \\
S_{\alpha\beta\delta} &= g_{\alpha\beta} (k_a - k_b)_\delta + g_{\beta\delta} (k_b - k_c)_\alpha + g_{\delta\alpha} (k_c - k_a)_\beta
\end{aligned} \tag{A5}$$

Comparing this to diagrams 12c) and 12d)

$$\begin{aligned}
-12c) &= -Cm_b^5 \frac{C_F C_A}{2} (ig)^4 \int d^4 k_b d^4 k_c N_{1c} \times \\
&\left[ \frac{i}{-2p(k_b + k_c) + (k_b + k_c)^2} \right]^2 \frac{i}{-2pk_c + k_c^2} \frac{-i-i}{k_c^2} \frac{-i}{k_b^2} \frac{-i}{(k_b + k_c)^2} \\
-12d) &= -Cm_b^5 \frac{C_F C_A}{2} (ig)^4 \int d^4 k_b d^4 k_c N_{2d} \times \\
&\frac{i}{-2p(k_b + k_c) + (k_b + k_c)^2} \left[ \frac{i}{-2pk_c + k_c^2} \right]^2 \frac{-i-i}{k_c^2} \frac{-i}{k_b^2} \frac{-i}{(k_b + k_c)^2}
\end{aligned} \tag{A6}$$

with the numerator factors

$$\begin{aligned}
N_{1c} &= \bar{u} \gamma^\alpha (\not{p} + \not{k}_a + m) (\not{p} + \not{k}_a + m) \gamma^\beta (\not{p} - \not{k}_c + m) \gamma^\delta S_{\alpha\beta\delta} u \\
N_{2d} &= \bar{u} \gamma^\alpha (\not{p} + \not{k}_a + m) \gamma^\beta (\not{p} - \not{k}_c + m) (\not{p} - \not{k}_c + m) \gamma^\delta S_{\alpha\beta\delta} u
\end{aligned} \tag{A7}$$

we have to show  $N_1 = N_{1c}$  and  $N_2 = N_{2d}$  to linear order in the integration. By power counting we must keep terms to the order  $k$  in the numerators in addition to the triple gluon vertex  $k$  dependence. The logarithmic terms arise dropping the  $k$  dependence everywhere in the numerators except in the triple gluon vertex  $S_{\alpha\beta\delta}$ . A simple calculation shows that the numerator factors for the logarithmic terms are zero. For the linear terms, a little more calculation gives

$$\begin{aligned}
N_1 &= 4m^2 \{ (k_a - k_b)_0 \bar{u} \not{k}_a u + 2(k_b - k_c)_0 \bar{u} \not{k}_c u + \\
&+ \bar{u} (\not{k}_b - \not{k}_c) \not{k}_a u + \bar{u} \not{k}_a (\not{k}_c - \not{k}_a) u - \bar{u} \not{k}_c (\not{k}_a - \not{k}_b) u - \bar{u} (\not{k}_c - \not{k}_a) \not{k}_c u \} = N_{1c}
\end{aligned} \tag{A8}$$

where the rest-frame condition was used. An entirely similar calculation gives  $N_2 = N_{2d}$  to linear accuracy. Thus the numerator factors are equal up to linear order in the integration, and equality (A3) is established to linear order. Hence we have shown the cancellation of the logarithmic and linear wave function renormalization pieces of group-5.

## REFERENCES

- [1] J. Chay, H. Georgi and B. Grinstein, *Phys. Lett.* **B247** (1990) 399; I. I. Bigi, N. G. Uraltsev, A. I. Vainshtein, *Phys. Lett.* **B293** (1992) 430; I. I. Bigi, M. Shifman, N. G. Uraltsev, A. I. Vainshtein, *Phys. Rev. Lett.* **71** (1993), 496; A. V. Manohar and M. B. Wise, *Phys. Rev.***D** **49** (1994), 1310.
- [2] R. Akhoury and V.I. Zakharov, *Nucl. Phys. Proc. Supp.* **A 54** (1997) 217 , hep-ph/9610492.
- [3] M. Beneke and V. M. Braun, *Nucl. Phys.* **B426** (1994) 301; I. I. Bigi, M. Shifman, N. G. Uraltsev, A. I. Vainshtein, *Phys. Rev.* **D 50** (1994), 2234; M. Beneke, V. M. Braun and V. I. Zakharov, *Phys. Rev. Lett.* **73** (1993) 3058.
- [4] The wave function renormalization of the initial heavy quark is another source of infrared sensitivity at the logarithmic and at the linear level. These also cancel against the radiated energy as we discuss in detail in the following sections, however for the purposes of the subsequent discussion, we will consider just the mass renormalization contribution.
- [5] J. D. Jackson, *Classical Electrodynamics* (1975), J. Wiley and Sons, New York.
- [6] B. R. Webber, *Phys. Lett.* **B339** (1994) 148; B. R. Webber and Yu. L. Dokshitzer, *Phys. Lett.* **B352** (1995) 415; R. Akhoury and V. I. Zakharov, *Phys. Lett.* **B357** (1995) 646.
- [7] R. Akhoury and V. I. Zakharov, *Phys. Rev. Lett.* **76** (1996) 2238.
- [8] T. Kinoshita *J. Math. Phys.* **3** (1962) 650; T. D. Lee and M. Nauenberg *Phys. Rev.* **133** (1964) 1549.
- [9] R. Akhoury, L. Stodolsky and V. I. Zakharov, **hep-ph/9609638**, To Appear in *Nucl. Phys. B*.
- [10] R. M. Doria, J. Frenkel and J. C. Taylor, *Nucl. Phys.* **B168** (1980) 93; C. Di'Lieto, S. Gedron, I. G. Halliday and C. T. Sachrajda, *Nucl. Phys.* **B183** (1981) 223.
- [11] R. Akhoury, M. G. Sotiropoulos and V. I. Zakharov, *Phys. Rev.* **D 56** (1997), 377.
- [12] M. Beneke and V. M. Braun, *Nucl. Phys.* **B454** (1995) 253.

# FIGURES

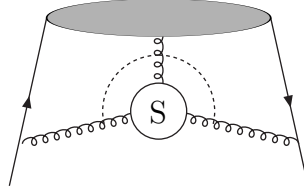


FIG. 1. The forward scattering amplitude for the heavy quark decay whose imaginary part gives the decay width. Shaded blob denotes the hard part, while S denotes the soft gluon interactions.

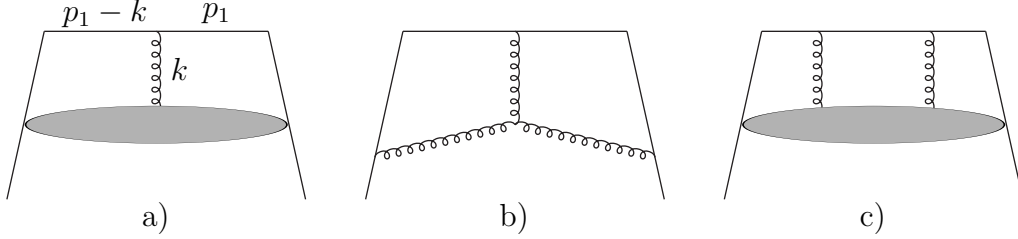


FIG. 2. a) Emission of a single gluon from the final state quark. The blob denotes all possible gluon self-interactions before coupling to the heavy quark. b) An example for the gluon self-interactions included in a). c) Two gluon emission from the final state quark.

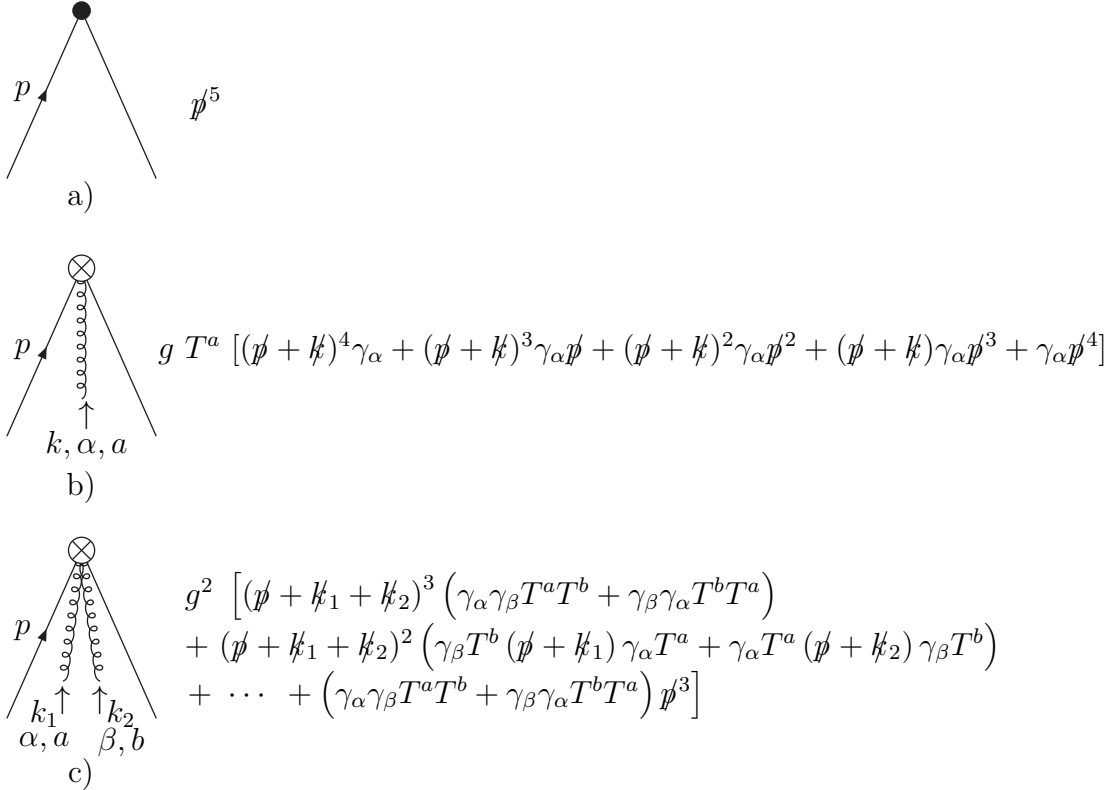


FIG. 3. a) leading effective vertex, b) single gluon effective vertex , c) double gluon effective vertex

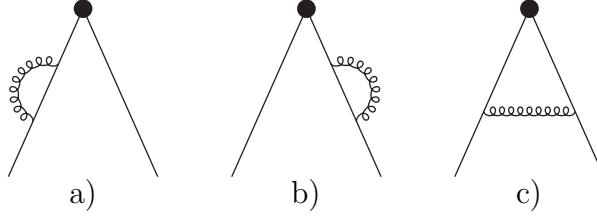


FIG. 4. Wave function renormalization and Bremsstrahlung diagrams to order  $g^2$ .

$$-i \frac{\partial}{\partial p_\nu} \text{---} \text{gluon loop} \text{---} = \text{gluon loop} \text{---} \text{---} \nu$$

FIG. 5. One-loop order Ward-like identity

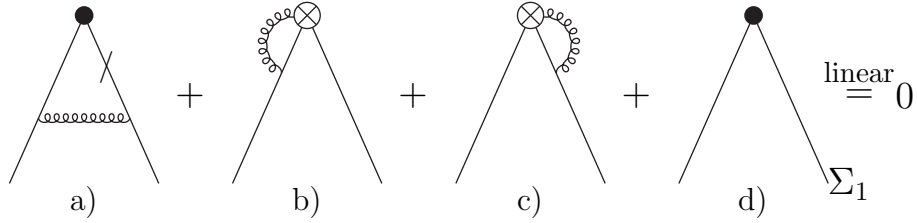


FIG. 6. Mass renormalization and the corresponding bremsstrahlung diagram to order  $g^2$ . Figure a) depicts the mass renormalization piece of the graph. The propagator with slash is cancelled by the expansion of the leading effective vertex. The subscript  $\Sigma_1$  of d) denotes the mass shift due to the order  $g^2$  self-energy correction.

$$\begin{aligned} -i\Sigma = & \frac{\text{gluon loop}}{-i\Sigma_1} + \frac{\text{gluon loop}}{-i\Sigma_{21}} + \frac{\text{gluon loop}}{-i\Sigma_{22}} + \frac{\text{gluon loop}}{-i\Sigma_{23}} \\ & + \frac{\text{gluon loop}}{-i\Sigma_{24}} + \frac{\text{gluon loop}}{-i\Sigma_{25}} \end{aligned}$$

FIG. 7. Self-energy corrections of order  $g^2$  and  $g^4$

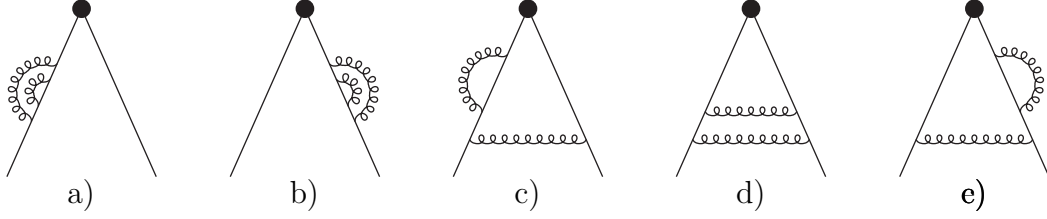


FIG. 8. The first group of 2-loop diagrams corresponding to  $\Sigma_{21}$ .

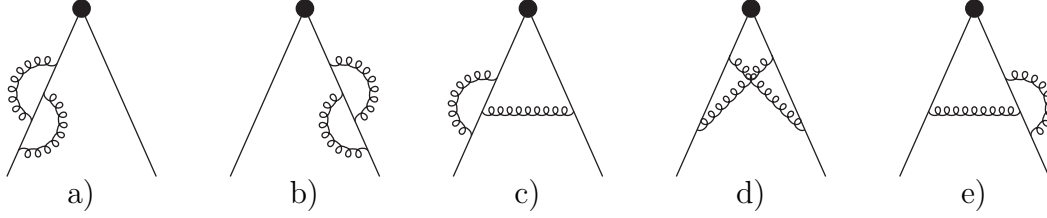


FIG. 9. The second group of 2-loop diagrams corresponding to  $\Sigma_{22}$ .

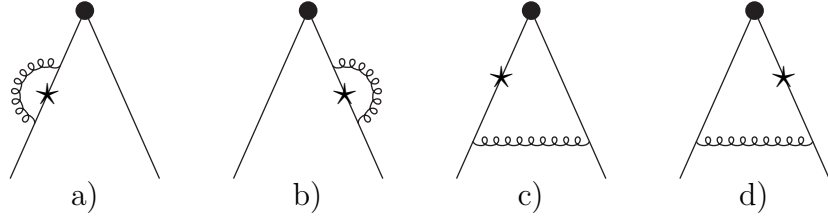


FIG. 10. The third group of 2-loop diagrams corresponding to  $\Sigma_{23}$ .

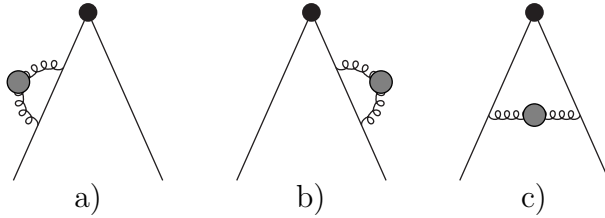


FIG. 11. The 4th group of 2-loop diagrams corresponding to  $\Sigma_{24}$ . The blob denotes fermion, gluon and ghost loops.

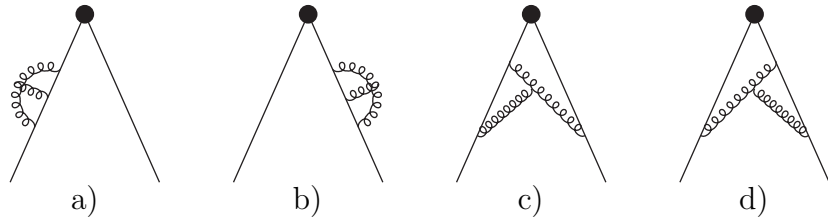


FIG. 12. The 5th group of 2-loop diagrams corresponding to  $\Sigma_{25}$ .

$$-i\frac{\partial}{\partial p_\nu} \text{---}\overbrace{\hspace{1cm}}^{\text{loop}}\text{---} = \text{---}\underbrace{\hspace{1cm}}_{\nu}^{\text{loop}}\text{---} + \text{---}\underbrace{\hspace{1cm}}_{\nu}^{\text{loop}}\text{---} + \text{---}\underbrace{\hspace{1cm}}_{\nu}^{\text{loop}}\text{---}$$

$$-i\frac{\partial}{\partial p_\nu} \text{ (diagram with two gluon loops) } = \text{ (diagram with one gluon loop and one gluon line) } + \text{ (diagram with one gluon loop and one gluon line) } + \text{ (diagram with one gluon loop and one gluon line) }$$

$$-i\frac{\partial}{\partial p_\nu} \text{---} \star \text{---} = \text{---} \star \text{---} + \text{---} \star \text{---}$$

c)

$$-i \frac{\partial}{\partial p_\nu} \text{---} = \text{---} \nu$$

[illegible]

FIG. 13. Two-loop order Ward-like identities

$$\begin{array}{c} \bullet \\ \diagup \quad \diagdown \\ \text{wavy line} \quad \text{wavy line} \end{array} + \begin{array}{c} \bullet \\ \diagup \quad \diagdown \\ \text{wavy line} \quad \text{wavy line} \end{array} + \dots = \frac{3}{4} [(Z^{-1} - 1)_{g^2}]^2 m_p^5$$

$$\text{triangle diagram} + \dots = \frac{1}{4} [(Z^{-1} - 1)_{g^2}]^2 m_p^5$$

$$\text{triangle with gluon loop on left} + \text{triangle with gluon loop on right} + \dots = -[(Z^{-1} - 1)_{g^2}]^2 m_p^5$$

FIG. 14. 1-particle reducible diagrams for wave function renormalization. The ellipsis denote all possible inclusion of mass counterterms.

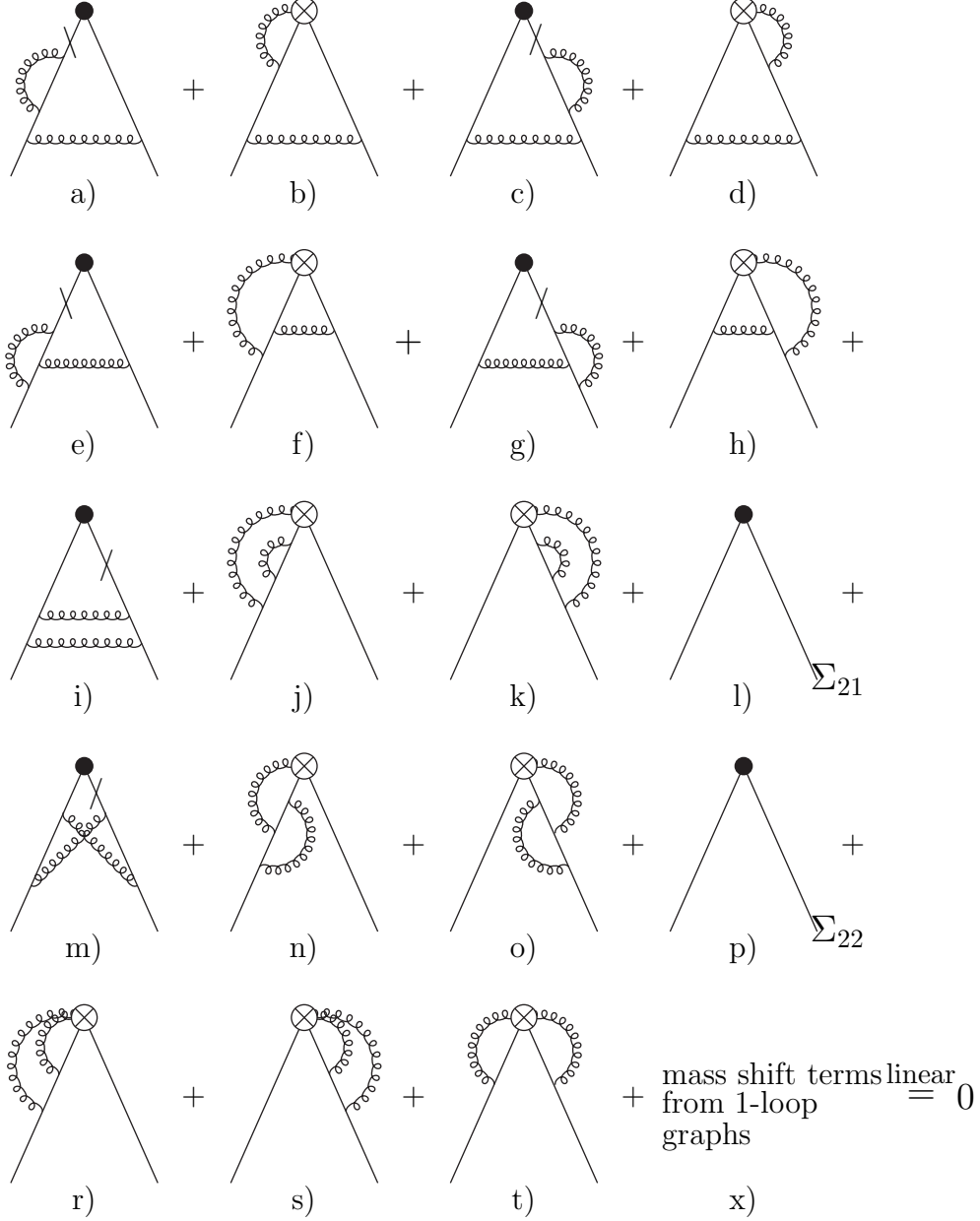


FIG. 15. Mass renormalization of order  $g^4$ : group-1 and group-2. The linear infrared sensitive mass renormalization pieces of the leading effective vertex graphs cancel with the corresponding single and double gluon vertex graphs and with  $g^4$  order mass shift terms from the 1-loop diagrams.

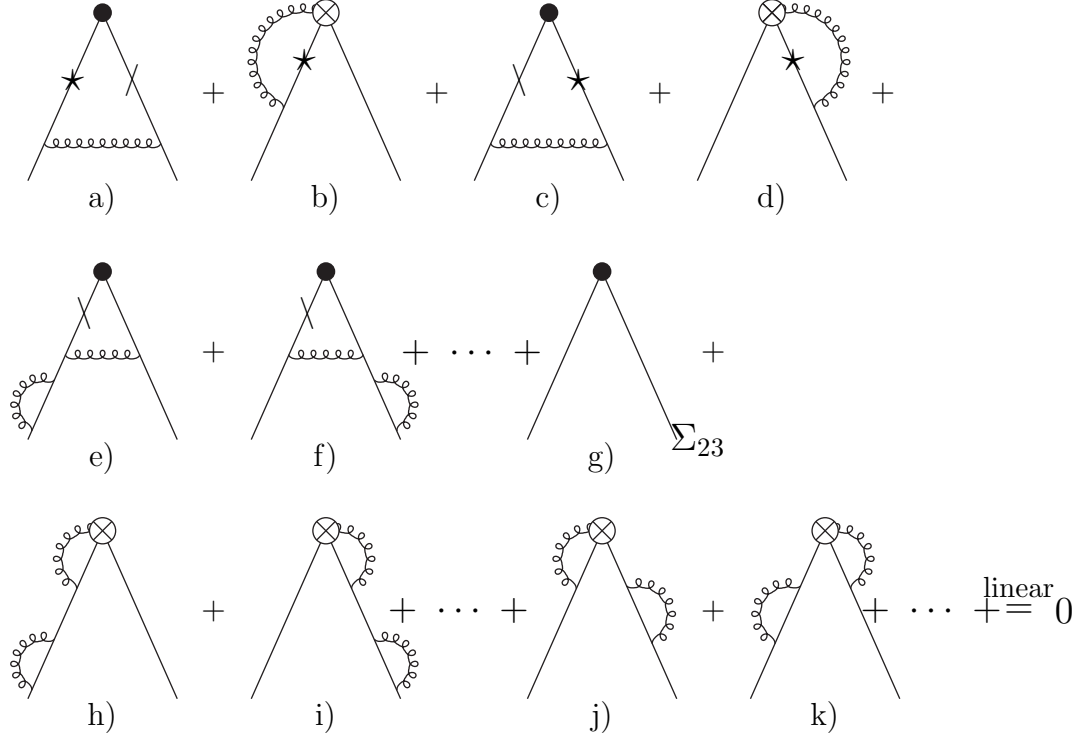


FIG. 16. Mass renormalization of order  $g^4$ : cancellation of linear mass terms between group-3 and the 1-particle reducible diagrams. The ellipsis denote inclusion of mass counterterms.

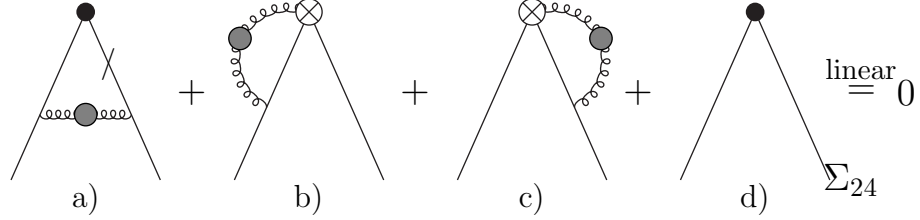


FIG. 17. Mass renormalization of order  $g^4$ : cancellation of linear pieces in group-4

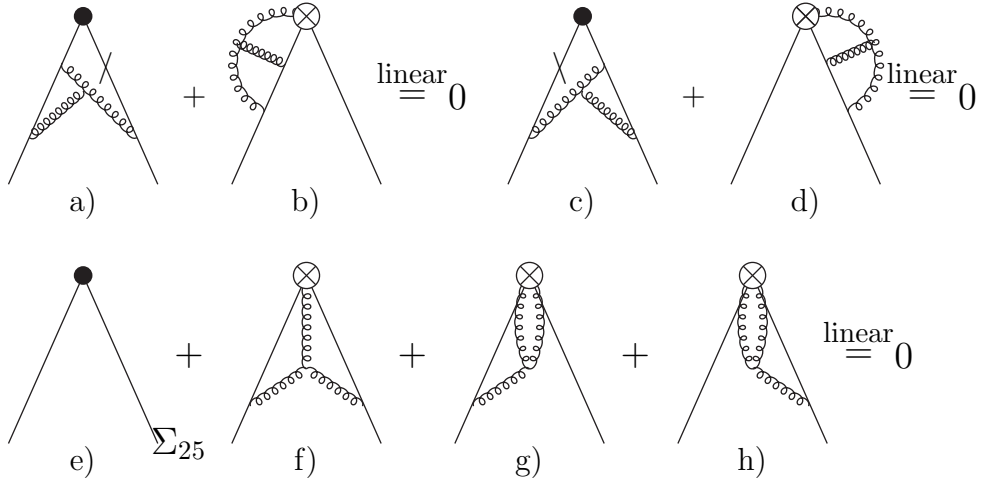




FIG. 18. Mass renormalization of order  $g^4$ : cancellation of linear terms in group-5.